ELECTROSPUN CELLULOSE FIBRES

FROM KRAFT PULP

by

Sang Ju Yeoh

B.A.Sc., University of British Columbia, 2007

A THESIS SUBMITTED IN PARTIAL FULFILLMENT OF
THE REQUIREMENTS FOR THE DEGREE OF

MASTER OF APPLIED SCIENCE

in

The Faculty of Graduate Studies

(Materials Engineering)

THE UNIVERSITY OF BRITISH COLUMBIA
(Vancouver)

September 2009

© Sang Ju Yeoh, 2009

ABSTRACT

Cellulose, the most abundant biomass extractable from wood, was generated in fibre form from kraft pulp by electrospinning, a fibre-producing process using electrostatic forces. Kraft pulping is the most dominant pulping technique in North America. Kraft pulp fibres (diam. 30μm) have a tensile strength of 700MPa and elastic modulus of 20GPa. In comparison, individual cellulose nanofibrils (diam. 5nm) have a tensile strength of 10GPa and elastic modulus of 150GPa. The strength displayed by cellulose nanofibrils suggests that the smaller fibre diameter could lead to a lower probability of including smaller flaw sizes in the fibre. Electrospinning has been successfully demonstrated as a one-step process to produce cellulose fibres directly from kraft pulp, thereby showing great potential for reducing cost and making the fibre-producing process more environmental friendly. Based on SEM and XRD, the electrospun fibres have a fibrillation-free, nano-filament structure with a seemingly cellulose I crystal structure, indicating significant potential for making crystalline cellulose fibres directly from kraft pulp. Contact angle measurements show that the electrospun fibres appear more hydrophobic than kraft pulp. The mechanical properties of the electrospun fibres have a large variation, suggesting the need for further process optimization. The ability to produce cellulose fibres directly from kraft pulp with improved moisture resistance and mechanical properties could potentially result in the development of more high value-added products for the Canadian pulp and paper industry, and perhaps even globally.

TABLE OF CONTENTS

LIST OF TABLES

LIST OF FIGURES

ACKNOWLEDGEMENTS

First, I wish to express my deepest heart-felt appreciation to my advisor, Dr. Frank Ko, for all the support, encouragement, and guidance that has allowed me to develop my technical proficiency and soft skills. I am very grateful to my co-advisor, Dr. Wadood Hamad, who was instrumental in establishing the scope of the study and supportive by making himself available to discuss the work during after-work hours. I would also like to thank Dr. Göran Fernlund and Dr. Walter Cicha for their constructive suggestions during the thesis writing.

Dr. S. Atifi, Dr. S. Su and Dr. C. Miao were very kind to train me on various characterization techniques including TGA, DSC, DP and contact angle measurements. M. Fletcher, J. Drummond and V. Lawrence provided assistance on SEM and confocal microscopy. Anita Lam deserves a special thank-you for her excellent guidance in the XRD analysis. Dr. J. Kadla and his group members, Reza, Jennifer and Carmen, were of great assistance, especially in establishing the NMMO process. Dr. Y. Wan and Dr. H. Yang were very helpful by offering ideas for the electrospinning setup.

Finally, I would like to express my gratitude to my parents, family members and friends in Malaysia and Canada for their continuing support and encouragement. A special recognition goes to Mdm. Wang for the great food and care, and, of course, for allowing her daughter to marry me!

DEDICATION

To my wife Tiffany

1   INTRODUCTION

1.1   Background Research

Why cellulose?

Cellulose, the world's most abundant biomass as well as a biodegradable and renewable polymer, is a major component in wood and other plant substances.[1]
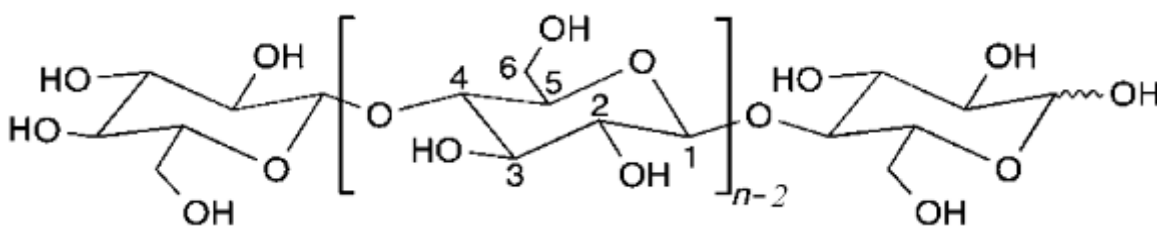
Figure 1. Molecular structure of cellulose

Natural cellulose fibres are hydrophilic. This renders them highly susceptible to loss of mechanical properties upon moisture absorption, which is a critical shortcoming for paper and board applications that require a high degree of dimensional stability and low hygroexpansivity. In addition, the highly polar nature of cellulose makes it poorly compatible with common non-polar polymers used in the production of textiles and composites. Furthermore, commercially-produced pulp fibres are seldom straight and continuous, and contain many deformations along their length – which manifest themselves in the form of dislocations, crimps and kinks in the fibre cell wall.

Deformations typically fall into two categories: (1) natural deformities in living trees, such as pits, or (2) induced through deliberate or incidental mechanical impact during processing. Induced deformations are primarily caused by axial compressive failure of the wall during pulp processing, which generally leads to structural changes in the fibre body and in the ultrastructure of the fibres. They do not allow the fibres' strength potential to be fully realized, and thus limit the applications of cellulose fibres in making load-bearing products at a wide range of environmental conditions. The ability to re-engineer and custom-design cellulose fibres to make them more moisture-resistant and mechanically stronger is a necessary first step towards developing high value-added products from a completely renewable resource, for advanced applications in electronic printing, packaging and structural materials having use in the automotive and aerospace industries.

Why kraft pulp?

Pulp is essentially cellulose in fibrous form. Pulping processes such as the kraft process remove most of the lignin and hemicellulose from raw wood, leaving behind cellulose as the main component in the pulp. Pulp has been widely used as the raw material for papermaking. Depending on the process that transforms natural woods into fibrous mass, pulp can be classified into three major categories, which are mechanical, chemi-mechanical, and chemical pulps. Among all the pulping techniques, chemical kraft pulping produces pulp of the highest quality in terms of mechanical strength, as shown in Table 1.[2] Chemical pulping involves the use of chemicals including sodium hydroxide and sodium sulfide to turn raw wood into pulp. Mechanical and chemi-mechanical pulping requires grinding of the raw wood to make pulp. Because mechanical grinding induces more physical damage and thus more defects to the fibre surface, chemical pulps are stronger than mechanical and chemi-mechanical pulps.[3] There are various factors that affect the mechanical properties of a fibre, including degree of polymerization, crystalinity, flaws, humidity, temperature and others. To produce regenerated cellulose fibres of high-tenacity, it is advantageous to begin with a raw material of the highest quality in terms of mechanical performance. In this case, kraft pulp is shown to be the best candidate material.

Table 1. Different pulping processes and the corresponding strength [2]

Classification	Process	Strength (MPa)
Mechanical	Stone Groundwood	350
	RMP	385
	TMP	455
Chemi-mechanical	Chemigroundwood	385
	Cold Soda	420
Chemical	**Kraft**	**700**
	Sulfite	630
	Soda	525

Because of the mechanical performance, kraft pulping accounts for two-thirds of the pulp production in British Columbia and North America. Considering that 3% of the Gross Domestic Product of British Columbia and Canada is provided by the forestry sector, the ability to develop value-added forestry products using kraft pulp is expected to have a positive impact on both the provincial and national economies.[4]

Why fibre?

From nature's point of view, the fundamental building blocks of living organisms are in fibrous forms. Naturally existing materials such as collagen, cellulose, chitin, silk and keratin are characterized by well-defined hierarchical fibrous structures down to the nano-scale. The gap between nano-materials and functioning macro-assemblies can be bridged by using materials in fibre form. Compared to other shapes such as spheres and cubes, a fibre has a significantly larger specific surface area. Fibres of high aspect ratio have been widely used for reinforcing purposes in polymer composites because of the efficient mechanical load transfer between the fibres and the polymer matrix, owing to the large specific surface area. Regenerated cellulose fibres have been used for various industrial applications, including textiles and precursors for carbon fibres. Lyocell and rayon are two examples of commercially available regenerated cellulose fibres. The electrospun cellulose fibre from kraft pulp differentiates itself from conventional regenerated cellulose fibres in that the electrospun fibre diameter can be significantly reduced to below a micrometer.

Why nanofibre?

As the fibre diameter decreases from micrometers to nanometers, the specific surface area is vastly increased. This intrinsic feature is of particular significance to many practical applications where high specific surface areas are required. The percentage of polymer molecular chains exposed on the fibre surface can be roughly expressed as 100 πd/D, where d and D represent the diameters of a polymer chain and the fibre, respectively.[5] This indicates that the percentage of polymer molecular chains exposed on the fibre surface increases with decreasing fibre diameter. As such, the ability to fabricate nanofibres with large specific surface areas provides an opportunity to effectively functionalize the fibres to enhance solubility, electrical conductivity, bio-compatibility, and other surface-dependent properties. Apart from surface chemistry, nano-scale surface features and topography have been shown to have a significant effect on numerous biological functions including cell adhesion, activation, proliferation, alignment and orientation.[6] The interest to regenerate cellulose on the nano-scale can be justified by the strength evidence observed in cellulose nanofibrils as shown in Table 2.[7,8,9] While molecular weight, crystalinity and molecular chain orientation are the major factors to the high strength of the nanofibrils, the small diameter – and hence less and smaller defects in the fibre - could also be a significant contributing factor. Cellulose nanofibrils, which measure 5nm in diameter on average, have a tensile strength of 10000 MPa[10], which is at least an order of magnitude higher than any other cellulose forms, including kraft pulp and Lyocell. There is a significant difference between the diameter and strength of nanofibrils

(5nm and 10000MPa) and Lyocell (7000nm and 386MPa). Electrospun fibres can have a

diameter ranging from several nanometers to micrometers, which fills the structural gap

between Lyocell and nanofibrils.[11]

Table 2. Structural and mechanical properties of different cellulose forms [7,8,9]

Property	Kraft Pulp	Cellulose Nanofibrils	Lyocell	Viscose	Cuprammonium
Diameter (nm)	30 000	5	7 000	110 000	100 000
Tensile Strength (MPa)	700	10000	400	145	132
Modulus (GPa)	20	150	13	4.5	1.9
Breaking Strain (%)	1	-	8	30	20
Average DP	1000	-	600	300	500

Why electrospinning?

While cellulose nanofibrils have a high tensile strength of 10 GPa, it is challenging to produce a functioning macrostructure from nanofibrils because of their discrete length (500nm). Electrospinning is capable of producing cellulose fibres smaller than 1000nm in diameter with continuous length.[12] Compared to micro-fibres, there is an order of magnitude increase in specific surface area in nano-fibres, allowing an efficient load transfer in composite applications. It has been shown that the macro- and micro-structure of polymeric fibres can be re-constructed to produce defect-free fibres using the electrospinning process, by manipulating the process parameters and the polymer solution chemistry.[13] In this study, the feasibility of using electrospinning as a one-step process to produce ultra-fine cellulose fibres directly from kraft pulp will be assessed for the first time.

1.2   Problem Statement

The conventional regenerated cellulose fibre production processes (e.g. viscose rayon) requires a multiple-step process (Figure 2) to convert raw pulp into dissolving pulp before regenerated cellulose fibres can be produced.[14] There is therefore a great interest to establish a more energy-efficient one-step cellulose fibre regeneration process directly from raw pulp. The electrospinning process has been successfully demonstrated as a direct one-step technique to produce cellulosic fibres from various cellulose sources including cellulose acetate, cotton linters, and fibrous cellulose CF-11 powders.[15] The aim of this study is to assess the feasibility of producing regenerated cellulose fibres directly from kraft pulp using the electrospinning process (Figure 2).

Mechanical strength and moisture resistance of pulp fibres are the two properties that are of great interest to the pulp and paper industry. Commercial pulp fibres are fibrillated, discrete and have many defects along the length, thus leading to a loss in mechanical performance for the pulp fibres. The ability to produce fibrillation-free, continuous-length, defect-free regenerated cellulose fibres would provide the potential to fully utilize the fibre strength. Natural pulp fibres are hydrophilic. Upon moisture absorption, pulp fibres experience a reduction in mechanical properties. In this study, experiments were carried

out to control the moisture resistance of the cellulose fibres via structural re-construction

using the electrospinning process.[16]
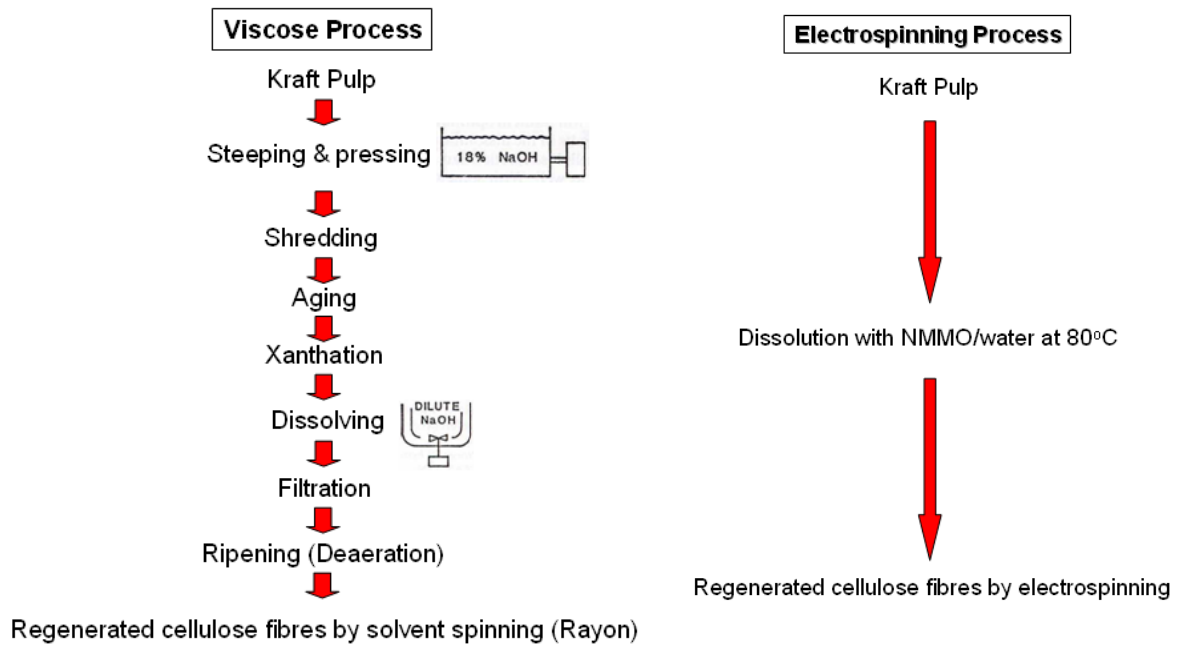
Figure 2. Process overviews of the viscose process (left) [14] and the electrospinning process (right)

1.3   Research Objectives

The research objectives are:

(1) To assess the feasibility of a more energy-efficient, cost-effective process using electrospinning to produce ultrafine cellulose fibres with controlled hydrophobicity directly from kraft pulp;

(2) To conduct a preliminary evaluation of the process-structure-property relationships of the electrospun cellulose fibres through various characterization techniques

2   LITERATURE REVIEW

2.1   Cellulose Dissolution Techniques

The existing and potential commercial applications for cellulose greatly depend on the cellulose dissolution techniques because the cost of cellulose solvents has a significant impact on the economic viability of the cellulose materials' commercial production.[17] Cellulose exists in four polymorphic forms, cellulose I, II, III, and IV, which can be characterized by X-ray diffraction.[18] Cellulose I is the crystal structure of native cellulose. Cellulose II is typically produced after native cellulose is regenerated or mercerized (treatment with sodium hydroxide). Cellulose III forms when native cellulose is treated with organic amines (RNH_2) or liquid ammonia (NH_3) followed by their anhydrous removal. Cellulose IV is a product of heat treatment of native cellulose with glycerol. These cellulose polymorphs have different solubilities in a particular solvent due to their different crystal structures. This literature review will discuss the solvent systems for cellulose that are used both commercially and in research.

2.1.1   N-methylmorpholine-N-Oxide (NMMO) And Water

N-methylmorpholine-N-oxide (Figure 3) is the only cellulose solvent used commercially to produce textile fibres Lyocell. This technology was established by American Enka and Eastman Kodak and later commercialized by Courtaulds.[19] NMMO is solid at room temperature (melting point 170°C). Hydration with one water molecule per NMMO molecule results in NMMO monohydrate (water content 13.3wt%) with a melting point of 74°C. Typically, the NMMO solvent system contains 85wt% of NMMO and 15wt% of water, thus requiring an elevated processing temperature (80-130°C) in the fibre spinning process.
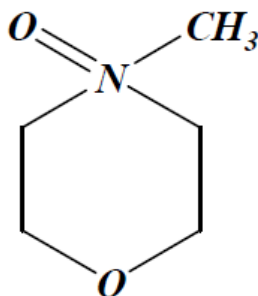
Figure 3. Chemical structure of NMMO

To prepare a cellulose solution using the NMMO solvent system, cellulose is added to a mixture of NMMO, water and propyl gallate. Propyl gallate, which acts as NMMO stabilizer, is a phenolic anti-oxidant for stabilizing the degree of polymerization (DP) of cellulose. During the dissolution process, the mixture is stirred and heated at a high

temperature ranging from 80 to 130°C. Upon complete dissolution, some of the cellulose is oxidized by NMMO to form a highly conjugated chromophore, which results in a clear brown solution.[20] Caution must be taken while heating the mixture above 150°C because rapid decomposition of NMMO can develop at such an elevated temperature and explosions may occur.[21]

While NMMO is an effective solvent for cellulose, there are a number of undesirable effects including loss of degree of polymerization, formation of colored oxidation products (such as chromophores which cause temporary or permanent fibre discoloration, lower fibre bleachability and formation of dark colored compounds in the spinning dope), and risk of explosions due to NMMO decomposition at high temperatures.[22] Despite the negative effects of the NMMO solvent system, it has the advantage of being an effective solvent recovery rate of 99.9% in the commercial Lyocell process. The closed-loop solvent spinning process makes it very cost-effective and environmentally friendly compared to other cellulose solvent systems.[23] Kulpinski demonstrated that submicron-scale cellulose fibres could be regenerated from cellulose/NMMO/water solution using the electrospinning process.[24] The electrospinning setup, fibre-forming conditions and structural characterization results via SEM were reported by Kulpinski.

2.1.2   N,N-dimethylacetamide (DMAc) And Lithium Chloride (LiCl)

McCormick and Turbak were the first to use the N,N-dimethylacetamide (Figure 4) and

lithium chloride solvent system to dissolve cellulose.[25] This solvent system was first used

in the dissolution of polyamides and chitin in 1972. The DMAc and LiCl cellulose solvent

system is commonly used for dissolving cellulose for the synthesis of cellulose derivatives

(such as cellulose acetate and cellulose nitrate) and for analytical purposes (such as gel

permeation chromatography).[26] Kim et al. reported that cellulose fibres could be

regenerated from cellulose/DMAc/LiCl solution using the electrospinning process.[27] The

effects of (1) solvent system, (2) degree of polymerization of cellulose, (3) spinning

conditions, and (4) water coagulation on the microstructure of the electrospun cellulose

fibres were reported by Kim et al.
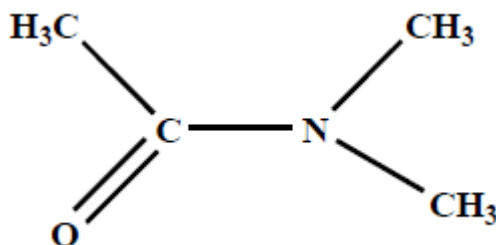
Figure 4. Chemical structure of N,N-dimethylacetamide[28]

The cellulose dissolution mechanism in this solvent system is understood to occur through

complex formation between the cellulose hydroxyl groups, DMAc and LiCl. During the

dissolution process, there must be no water in the solvent system. In the presence of water,

the hygroscopic nature of both DMAc and LiCl accelerates polymer aggregate formation

and prevents the complex formation between cellulose and the solvent system. The first

step to dissolving cellulose in this solvent system is to soak oven-dried cellulose in DMAc.

The DMAc/cellulose mixture is distilled in an inert gas environment at $165^{o}C$ for 30

minutes. After cooling the mixture down to $100^{o}C$, 8wt% of LiCl is added to the mixture,

which is stirred at $80^{o}C$ for 40 minutes to achieve complete cellulose dissolution. For

cellulose with a DP of 130 and 1700, complete dissolution is reported for cellulose

concentrations up to 15wt% and 4wt%, respectively. Depending on the cellulose DP,

undissolved and swollen cellulose fibres are observed when the cellulose concentration

exceeds the critical dissolution concentration.[29,30]

One advantage of using the DMAc/LiCl solvent system is its chemical stability. Unlike

the NMMO/water solvent system, no loss in DP of cellulose was observed in the solution

after several years at room temperature. McCormick et al. reported a 2% decrease in

relative viscosity of cellulose solutions in 9% LiCl/ DMAc over 30 days, which they

attributed to changes in inter- and intra-molecular hydrogen bonding.[31]

2.1.3 Ionic Liquids

Ionic liquids are a class of salts that exists in liquid state at a relatively low temperature (less than 100°C). The ability to dissolve both polar and non-polar compounds renders ionic liquids important in many chemical processes.[32] Ionic liquids have several other desirable properties including zero or low vapor pressure, high thermal stability, large liquid range, wide electrochemical window, low melting point, and convenient recyclability.[33] Because of these properties, ionic liquids are called "green" solvents. Furthermore, the properties of ionic liquids can be modified by altering their anionic and/or cationic structures. Ionic liquids have been shown to be promising solvent systems for biopolymers such as carbohydrates[34] and enzymes.[35] The major disadvantage of using ionic liquids as cellulose solvents is their high cost, which prevents them from being used on a commercial scale to produce commodity regenerated cellulose fibres.

The first attempt to dissolve cellulose using ionic liquids is believed to have been carried out in 1934 by Graenacher using molten N-ethylpyridinium chloride in the presence of nitrogen-containing bases. Rogers et al. later demonstrated that hydrophilic ionic liquids including 1-allyl-3-methylimidazolium chloride [AMIM][Cl] and 1-butyl-3-methylimidazolium chloride [BMIM][Cl] (Figure 5) could dissolve cellulose.[36] [BMIM][Cl] can dissolve up to 25wt% of cellulose under heating. The effectiveness in breaking the extensive hydrogen-bonding network in cellulose could be due to the high

chloride reactivity and chloride concentration in [BMIM][Cl]. As shown in Table 3, the

choice of ionic liquids and heating can significantly affect the solubility of cellulose.
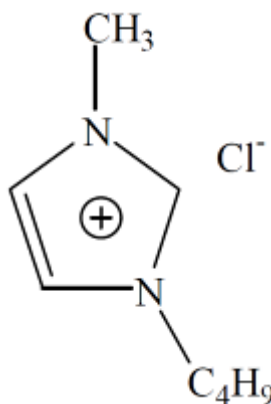
Figure 5. Chemical structure of 1-butyl-3-metylimidazolium chloride [BMIM][Cl][37]

Table 3. Cellulose dissolution in [BMIM] ionic liquids[38]

Ionic Liquid	Method	Solubility (wt%)
[BMIM]Cl	Heat at 100°C	10
[BMIM]Cl	Heat at 80°C + sonication	5
[BMIM]Cl	Microwave heating 3-5 pulses	25 (clear viscous solution)
[BMIM]Br	Microwave heating 3-5 pulses	5-7
[BMIM]SCN	Microwave heating 3-5 pulses	5-7
[BMIM][BF$_4$]	Microwave heating 3-5 pulses	Insoluble
[BMIM][PF$_6$]	Microwave heating 3-5 pulses	Insoluble

Cellulose solutions prepared using ionic liquids can be regenerated in water, ethanol or

methanol. The regenerated cellulose has nearly the same degree of polymerization and

polydispersity as the native cellulose. The ionic liquids can be recycled and reused

through various means, including salting out, reverse osmosis, evaporation, and ionic

exchange.[39] Viswanathan et al. reported that cellulose and cellulose-heparin composite

fibres could be prepared from room temperature ionic liquid solvent by electrospinning.[40]

The fibre-forming conditions and structural characterization (using SEM) of the

electrospun fibres from ionic liquid-based cellulose solutions were reported by

Viswanathan et al.

2.1.4 Ammonia/ Ammonium Thiocyanate

Ammonia/ammonium thiocyanate (NH_3/NH_4SCN) was demonstrated to be an effective cellulose solvent by Cuculo and Hudson in 1980. Thermally reversible gelation and fibre formation were also demonstrated in their studies. The advantages of using this solvent system include low production cost and readily available components, such as ammonia and ammonium thiocyanate.[41,42] The solvent system can be handled conveniently because of its low boiling point at about 70°C. It was also reported that there was no degradation of cellulose and no apparent reaction between the cellulose and the solvent. To prepare the solvent, NH_4SCN is first dried and purified by re-crystallization from NH_3. The NH_3/NH_4SCN is prepared by dissolving NH_3 with dried and purified NH_4SCN to obtain a composition of 24.5/75.5 w/w.[43] The disadvantage of this solvent system is that it requires a condensation step while preparing the solvent with NH_3. In the use and storage of this solvent system, its evaporation must be minimized to prevent subsequent NH_4SCN crystallization.[44]

2.1.5 Amine Salts

A two-component system consisting of hydrazine (NH_2-NH_2) or ethylenediamine (NH_2-CH_2-CH_2-NH_2) and several thiocyanate salts including LiSCN, NaSCN, or KSCN that can be used as cellulose pulp solvent was reported by Hattori et al.[45] Cellulose I, II and III can be effectively dissolved in the amine-salt solvents. The disadvantage of this solvent system is that it requires a high concentration of the amine salts (40-50%) to dissolve up to 20wt% of cellulose and hydrazine is very toxic.

The amine salt solvent system involves a temperature cycling step to ensure cellulose dissolution. In a typical temperature cycling procedure, cellulose pulp is combined with a thiocyanate salt and amine (hydrazine or ethylenedimine) solvent in a sealable polyethylene bag in the presence of nitrogen. The mixture is then cooled down to -10ºC for about an hour and then warmed up to 50ºC with intermittent shearing for 30 minutes. The temperature cycling step is repeated several times for the complete dissolution of cellulose pulp. Hattori et al reported that cellulose (DP 210) solution with a concentration of 18% w/w can be easily prepared by using this technique. Hattori also reported that the mixture of hydrazine or ethylenedimine and NaSCN as cellulose solvent has the highest dissolving power among the mixtures (Table 4). Frey et al. demonstrated that cellulose/ethylenediamine/KSCN solutions could be electrospun into nanofibres using the electrospinning process. [46] The electrospinning process conditions and structural

characterization (using SEM) of the electrospun fibres from amine salt-based cellulose

solutions were reported by Frey et al.

Table 4. Cellulose dissolution in the amine salt solvent systems

Solvent system	Salt Solubility (g/100g of amine)	Cellulose Solubility (wt%)
NH_2NH_2/NaSCN	91	18
NH_2NH_2/KSCN	200	14
NH_2NH_2/NaI	66	16
$NH_2CH_2CH_2NH_2$/NaSCN	86	18
$NH_2CH_2CH_2NH_2$/KSCN	81	14
$NH_2CH_2CH_2NH_2$/Ca(SCN)$_2$	Insoluble	Insoluble

2.2   Cellulose Dissolution In N-Methylmorpholine-N-Oxide System
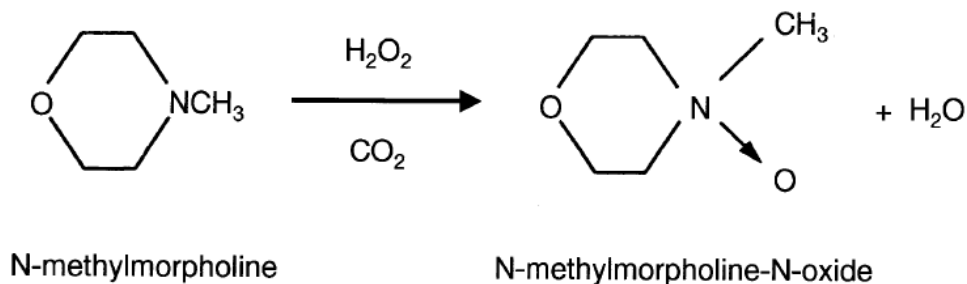
Figure 6. Formation of NMMO

NMMO is produced from the oxidation of the ternary amine N-methylmorpholine using hydrogen peroxide (Figure 6).[47] Pure NMMO has a melting point of 170°C. NMMO monohydrate (NMMO.H_2O, water content 13.3wt%) has a melting point of about 74°C and dissolves cellulose more readily. The strong N-O dipoles of NMMO in aqueous state are key to the capability of NMMO to physically dissolve cellulose without complexation (formation of a weak reversible chemical bonds between cellulose and another compound), or special activation/derivatization (formation of a similar chemical structure with additional functional group(s), for example acetylation of cellulose to form cellulose acetate).[48]

Figure 7. Phase diagram for cellulose/NMMO/water system[49]

Figure 7 shows the cellulose solubility in the binary NMMO–water mixture. The phase diagram depicts a relatively small region where cellulose is completely dissolved in the highly concentrated NMMO. The NMMO dissolution process begins with a composition (slurry) outside the small region of complete dissolution. Complete wetting and swelling of the cellulose must be ensured while preparing the slurry. To reach the composition of the region of complete dissolution (13–15 wt% water), water is removed from the slurry at reduced pressure and elevated temperature. Upon complete dissolution, a homogeneous and viscous cellulose solution is formed.

2.2.1 Cellulose Dissolution Mechanism In NMMO/water system

While the NMMO technique is well established and used commercially, with an annual output of 100 ktons Lyocell fibres, the dissolution mechanism and the structure of cellulose–NMMO solutions are not well understood. NMR indicates that neither cellulose derivatization nor complexation takes place with NMMO.[50] However, hydrogen bonds are expected to form between the oxygen of the strong N-O dipoles in NMMO and other hydroxyl-group-containing compounds including water and cellulose.[51] It follows that during cellulose dissolution in the NMMO/water solvent system, water and cellulose must compete against each other to bond with NMMO molecules, which seem to prefer water. Therefore, homogeneous cellulose solutions can only be obtained with a limited amount of water. With NMMO, the disruption of the hydrogen bond system in cellulose is likely to be caused by the formation of hydrogen bond complexes between the solvent and cellulose hydroxyl groups.[52] The successful application of stabilizers (antioxidants such as propyl gallate) that minimize the radical decomposition of NMMO and cellulose chain scission at the necessary high temperatures have led to the technical breakthrough with NMMO.[53]

In other solvent systems (for example DMAc/LiCl), cellulose dissolution cannot be achieved in one single step. This is because the highly ordered regions of the native cellulose I hinder access of the solvent molecules to the cellulose hydroxyl groups.

Consequently, an activation process using thermo-mechanical treatments or highly polar compounds is introduced to break down the cellulose hydrogen bond system. Krässig reported that such structural changes improve the accessibility to the native cellulose fibrils and chains of the solvent molecules.[54]

2.3   **Routes to Regenerated Cellulose Fibres**

As discussed in the previous sections, a number of cellulose solvent systems have been developed. However, only three cellulose fibre processing methods, which are the cuprammonium rayon process, the viscose rayon process, and the Lyocell process, were commercialized.

The first commercial regenerated cellulose fibres were produced via the cuprammonium rayon process. The German chemist Matthias Eduard Schweizer reported in 1857 that cotton, linen cellulose and silk could be dissolved in cuprammonium solution (ammonial copper oxide solution) at room temperature.[55] In 1890, a French chemist named Louis Henri Despeissis was the first to demonstrate the ability to regenerate fibre from cellulose dissolved in cuprammonium solution.[56] In 1907, the cuprammonium process began to face stiff competition from the viscose process and it became clear in 1909–1910 that the cuprammonium process could not compete economically against the new viscose process. Furthermore, it was inferior in quality to the cellulose nitrate silk. Consequently, the cuprammonium process was phased out and replaced by the viscose process after 1909.

The viscose rayon process was first patented by Cross and Bevan in 1893. Samuel Courtauld successfully commercialized it in 1907 and consequently the viscose rayon

fibres became hugely popular in the textile industry. In 1910, DuPont, Tubize and Belamore began viscose rayon production in America and the production rate reached 2,000,000 lb/year.[57] However, the viscose process suffers from a number of hazards, including carbon disulphide and hydrogen sulphide emissions. Their toxic effects would cause deep unconsciousness and even death among workers in the viscose rayon industry. With a flashpoint below -30°C, carbon disulphide is a fire and explosion hazard. The acids and alkalis used in the viscose process also were hazardous to the workers.

The Lyocell process or N-Methylmorpholine-N-Oxide (NMMO) process was commercialized quite recently to produce regenerated cellulose fibres. In 1984, the first commercial samples were produced and Lyocell fibre has become increasingly popular ever since. In 1992, Courtaulds began commercially producing staple cellulose fibres. The impact of the Lyocell process was to produce regenerated cellulose fibres having greater cost-efficiency and mechanical performance, while the process is more environmentally friendly process than the viscose rayon process. In summary, the NMMO cellulose regeneration process is more modern, efficient, and nonpolluting than any of the other ones.[58]

2.3.1 Cuprammonium Process

In the cuprammonium process, cellulose is first dissolved in an aqueous ammonial copper hydroxide solution and is extruded through a spinneret to form fibres. Removal of fatty and resinous materials is carried out before cellulose dissolution by washing to accelerate the dissolution process.[59] The undissolved matters are removed by filtering the solution through sand and asbestos. The filtered solution is extruded into an acid bath (e.g. formic acid, hydrochloric acid or citric acid) that contains alcohol and concentrated cresol solution. When the solution comes into contact with the bath, cellulose precipitates immediately to form hard solid fibres. The fibres are then stretched in dilute hydrochloric acid using a winder, spool and drum. The remaining copper and ammonia in the fibres react chemically with the hydrochloric acid to form easily removed copper chloride and ammonium chloride. The washed fibres are dried and reeled. Figure 8 depicts the multi-step cuprammonium processing route developed by Despeissis.[60]
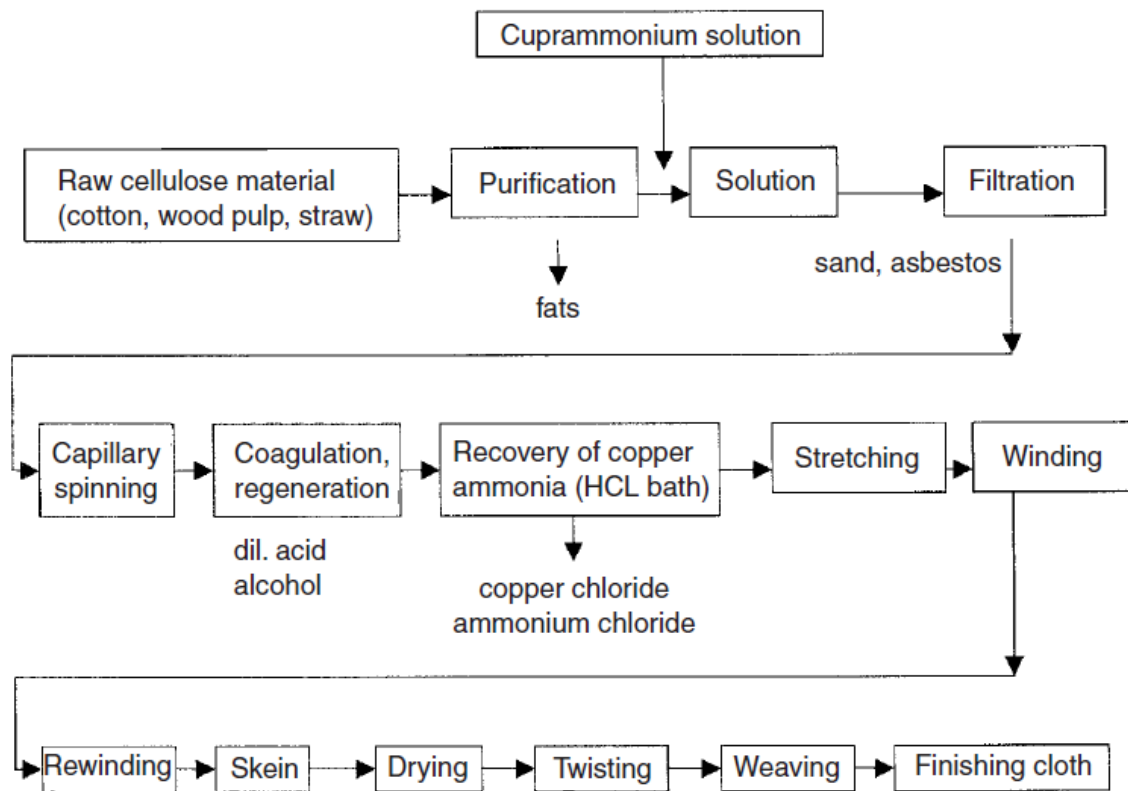
Figure 8. Regenerated cellulose production by the cuprammonium process[61]

2.3.2   Viscose Process

The viscose process begins by first steeping the pulp in an aqueous solution of 17-19% sodium hydroxide. The pulp fibres swell and are converted to sodium cellulosate (alkali cellulose or white crumb). The swollen mass is then pressed to attain a desired ratio of cellulose to alkali and is then shredded to provide a uniform surface area, for reaction in the following processing steps. Sodium cellulosate is depolymerized by oxidation through aging under controlled time and temperature. This is then followed by the conversion to sodium cellulose xanthate via a reaction with carbon disulphide. The xanthate is dissolved in dilute sodium hydroxide to form viscose. The orange viscous solution is filtered, deaerated (air removal), and ripened to the optimum salt index for spinning. The solution is extruded through a spinneret into a bath containing sulphuric acid, sodium sulphate, zinc sulphate and water to form the rayon fibres. Lastly, the fibres are washed to remove the acid, chemically treated to desulphurize and bleached, before final washing and application of a processing finish.[62]

2.3.3 Lyocell Process

The Lyocell process was developed to produce regenerated cellulose fibres that have a better cost-performance profile than viscose rayon. Other reasons include (1) the demand to increase the use of renewable resources as the raw materials and (2) to have a more environmentally friendly process involved in the fibre production. The main application of the Lyocell fibres is in the textile industry for making fabrics. As the performance of Lyocell fibres are continually enhanced through research and development, other non-textile end-uses, such as nonwoven fabrics and papers, are also being developed.

Lyocell is produced from wood pulp derived from sustainably managed forests. The wood pulp is first dissolved in a heated solution of N-methylmorpholine oxide (NMMO) to obtain a spinning dope. The spinning dope is highly viscous at its operating temperature (90–120°C) and must be processed in high-pressure equipment similar to that used in melt polymer systems. The spinning dope is then mechanically spun into fibres by coagulating in a water or water/NMMO bath. At the same time, the solvent is extracted as the fibres are washed in the bath. The manufacturing process is a closed-loop process designed to recover >99% of the solvent NMMO. The solvent itself is non-toxic and all the effluent produced is nonhazardous. Figure 9 is a schematic that describes the Lyocell spinning system established by Clarence McCorsley in 1979.[63]
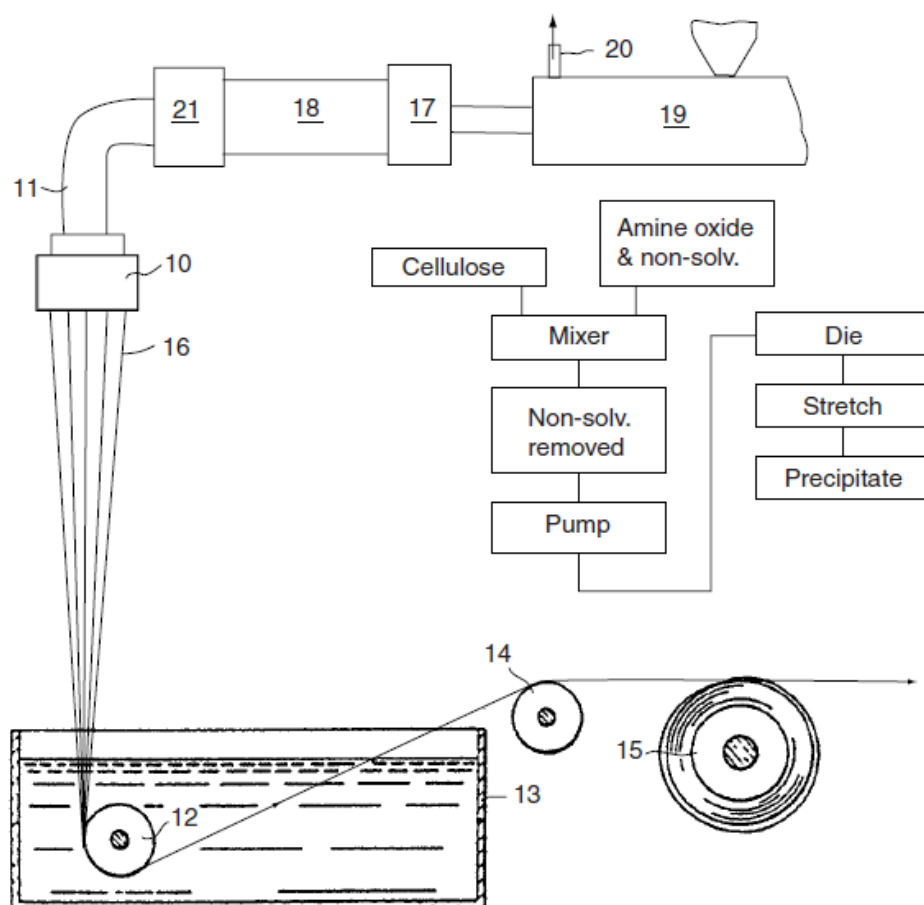
Figure 9. Clarence McCorsley's Lyocell spinning system [63]

As a cellulose fibre, Lyocell is fully biodegradable, absorbent and its surface properties can be modified through the use of enzymes or chemical finishing techniques. It has a relatively high wet and dry strength, which allows for the production of finer yarns and lighter fabrics. Fibrillation is a common issue that Lyocell shares with other cellulose fibres, including cotton and rayon. Fibrillation tends to occur when the wet fibre is abraded and the fibrils on the surface begin to peel away. The ability to better control the fibrillation behavior is a major area of continuing research.[64]

2.3.4 Electrospinning Process

Electrospinning has been widely investigated as a technique for fabricating continuous defect-free fibres.[65] The macro- and micro-structure of the fibres, which are regenerated from polymer solutions by electrospinning, can be re-constructed through manipulating the chemistry of the polymer solutions.[66] The first patent on the electrospinning process was given to Formhals in 1934.[67] In fact, the first electrospun fibres by Formhals were made from cellulose acetate, a cellulose derivative. In the past 50 years, a number of solvents for cellulose have been developed and used in wet- and dry-jet spinning processes.[68] The cellulose solvents that were investigated for electrospinning cellulose include NMMO[69,70,71], LiCl/DMAc[72], ionic liquids[73], and ethylene diamine/KSCN[74]. Table 5 summarizes the solvent systems and processing conditions used to produce electrospun fibres from cellulose solutions. While it has been demonstrated that cellulose fibres can be electrospun from cellulose solutions, there are no reports of producing electrospun fibres directly from kraft pulp. In conventional regenerated cellulose fibre processes such as the viscose process, raw pulp has to be converted into dissolving pulp. In this study, the pulp conversion step is eliminated and the direct production of cellulose fibres from kraft pulp using the electrospinning process is investigated. The ability to produce cellulose fibres from kraft pulp using a one-step process would have significant potential for reducing the regenerated cellulose fibre production costs and finding new product development routes for kraft pulp manufacturers. Furthermore, there has been no

discussion in the previous studies of the physical (e.g. hydrophobicity) and mechanical properties of the electrospun cellulose fibres. In this research, the hydrophobicity and mechanical properties of the electrospun cellulose fibres from kraft pulp were characterized.

Table 5. Summary of electrospinning conditions used to produce fibres from cellulose solutions

Solvent	Cellulose	Coagulant	Fibre diameter	Reference
NMMO/water	DP210, 9wt% DP1140, 1-3wt%	Rotating collector into water at $10^{o}C$	750nm	70
NMMO/water	DP670, 4wt%	Not specified	90-250nm	69
NMMO/water	DP800, 2wt%	Water	200-500nm	71
ED/KSCN	DP140, 8wt% DP940, 3wt%	Not specified	3 microns 100-1000 nm	74
LiCl/DMAc	DP1140, 1-3wt%	Heated rotating collector into water	250-750nm	72
bmIm/Cl or emIm/Ba	10wt%, DP not specified	Ethanol	500nm-10 microns	73

2.4   **Nanofibre Technology**

2.4.1   **What Is Nanofibre Technology?**

Nanofibres are a class of nanomaterials characterized by an aspect ratio greater than 1000:1 and high flexibility. According to the definition of nanomaterials by the National Science Foundation, only fibres with diameters equal to or less than 100 nm can be strictly classified as nanofibres. Nanofibres have many potential applications ranging from high-speed chemical sensors to bullet-proof vests, owing to their high longitudinal strength, large specific surface area, and flexibility.[75] Figure 1 shows an SEM image of electrospun cellulose acetate (CA) submicron-scale fibres with an average fibre diameter of 612 nm from a 24wt% CA/acetone/dimethylformamide solution.[76]
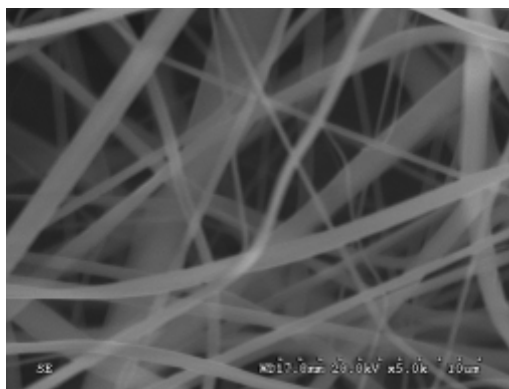
Figure 10. SEM image of electrospun cellulose acetate (CA) submicron-scale fibres [76]

A number of techniques such as melt-blowing, phase separation, self-assembly, template assembly, and electrospinning have been used for fabricating nanofibres. Electrospinning

has attracted the most interest, both from industry and academia because of its simplicity, cost-effectiveness, and ability to produce continuous nanofibres of various materials including polymers and composites. Reneker et al. reported the ability to fabricate polymer nanofibres with a diameter of 3 nm, and thus involving only 6 or 7 molecules along the diameter of the nanofibre.[77] In 2006, Ko and Gogotsi demonstrated the ability to coelectrospin nanocomposite fibres using spider silk reinforced with carbon nanotubes.[78] In addition, electrospinning is the only existing technology that shows promise for further development of large-scale continuous nanofibres production for industrial applications.[79]

2.4.2 Nanofibre Fabrication Techniques

Composite Spinning (Island in the Sea)

Sea–island-type conjugate spinning involves extruding two polymer components together from a spinning die. The island fibres are arranged in a sea component that is later removed by extraction. Nakata et al. reported that continuous PET nanofibres having a diameter of 39 nm could be obtained by sea-island-type conjugate spinning from the flow-drawn fibre, with further drawing and removal of the sea component. Figure 11 shows a TEM image of a PET island fibre and Nylon-6 sea produced by conjugate spinning and flow drawing.[80]
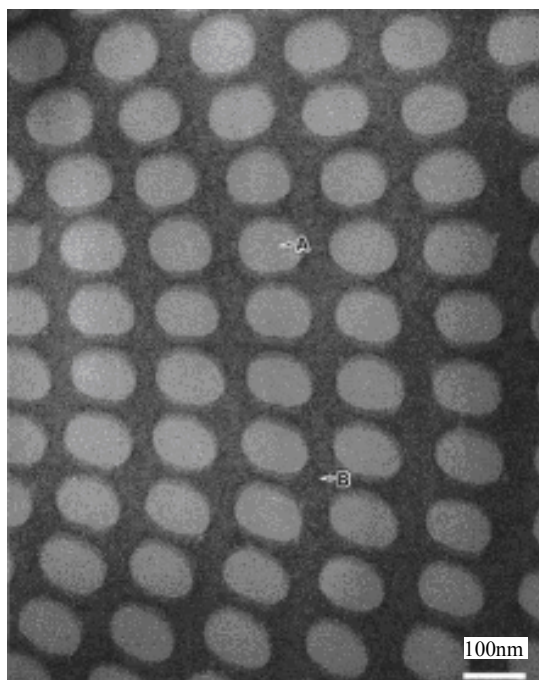
Figure 11. Cross-sectional TEM image of conjugated-spun and flow-drawn fibre: A) PET island fibre. B) nylon-6 sea. [80]

Chemical Vapour Deposition (CVD)

In the CVD process, a substrate is exposed to one or more volatile precursors, which react and/or decompose on the substrate surface. The desired deposit thus is synthesized there. Volatile by-products are produced during the process and are removed by gas flow through the reaction chamber. The various structural forms of materials that can be produced via CVD include monocrystalline, polycrystalline, amorphous, and epitaxial. Silicon, carbon fibre, carbon nanofibres, filaments, and carbon nanotubes are some examples of materials that can be fabricated using CVD.[81]

Drawing

Drawing is a process similar to dry spinning in the synthetic fibre industry, which can make long, continuous single nanofibres. However, only a viscoelastic material that can undergo strong deformations while being cohesive enough to support the stresses developed during pulling can be made into nanofibres via this technique.[82]

Template synthesis

In the template synthesis method, a nanoporous membrane is used as a template to make nanofibres of a solid fibril or a hollow tubule. The materials that can be used to grow tubules and fibrils by template synthesis include electronically conducting polymers, metals, semiconductors, and carbon. However, single continuous nanofibres cannot be fabricated by this method.[83]

Self-assembly

Self-assembly is a process whereby individual, pre-existing components organize themselves into desired patterns and functions. Niu et al reported that one-dimensional composite nanofibres with narrow dispersity, high aspect ratio and high processibility could be fabricated by head-to-tail self-assembly of rod-like viruses, assisted by aniline polymerization. The potential applications of these composite nanofibres include electronics, optics, sensing and biomedical engineering.[84]

Melt blown technology

The melt blown technology involves producing fibres in a single step by extruding a polymer melt through an orifice die and drawing down the extrudate with a jet of hot air (typically at the same temperature as the molten polymer). The air exerts a drag force that attenuates the melt extrudate into fibres, which are then collected a few feet away from the die in the form of a non-woven mat. [85]

Electrospinning

Electrospinning is a well-established process for producing ultra-fine fibres, first patented in 1934 by Formhals using cellulose acetate.[86] The process currently produces micron scale fibres at a commercially viable level using electrostatic forces to pull fibres from a capillary containing polymer solution.   According to Deitzel et al., the technique can be

considered a variation of the electrospraying process.[87] The polymer solution consists of a predetermined mixture of polymer suspended in solvent. A drop of polymer solution forms at the tip of the capillary due to gravity and is held in place by surface tension. Formation of the fibre begins when the electrostatic force is greater than the surface tension of the droplet. The fibre is formed as the ejection jet stream is narrowed by increasing surface charge density, which results from the evaporation of the solvent. Nanofibre fabrication by electrospinning will be described in greater detail in the following section.

2.4.3   Nanofibres Via Electrospinning Process

The electrospinning process utilizes electrostatic forces in the fibre formation process, which is different from conventional fibre spinning techniques (melt, dry or wet spinning) that rely on mechanical forces to produce fibres by extruding the polymer melt or solution through a spinneret and subsequently drawing the resulting filaments as they solidify and coagulate. Electrospinning involves the application of an electric field between a capillary tip and a grounded collector via a high-voltage source. A pendent droplet of polymer solution at the capillary tip is transformed to a hemispherical shape and then into a conical shape (known as a Taylor cone) by the electric field. When the intensity of the electric field causes a larger effect than the surface tension of the polymer solution, the solution is ejected towards the grounded metallic collector. If the concentration of the solution is low, the jet breaks up into droplets. However, when the viscosity is high enough, which indicates entanglements of the polymer chains, a continuous jet is formed. A series of electrically induced bending instabilities in the air results in stretching and elongation of the jet in a cone-shaped volume. Rapid evaporation of the solvent during the elongation process reduces the fibre diameter. The non-woven mat collected on the grounded surface contains continuous fibres at micron to nano-scale.[88,89] The basic electrospinning setup consists of a high voltage power supply, an electrode, a glass syringe/pipet filled with polymer solution and a grounded target as shown in Figure 12.
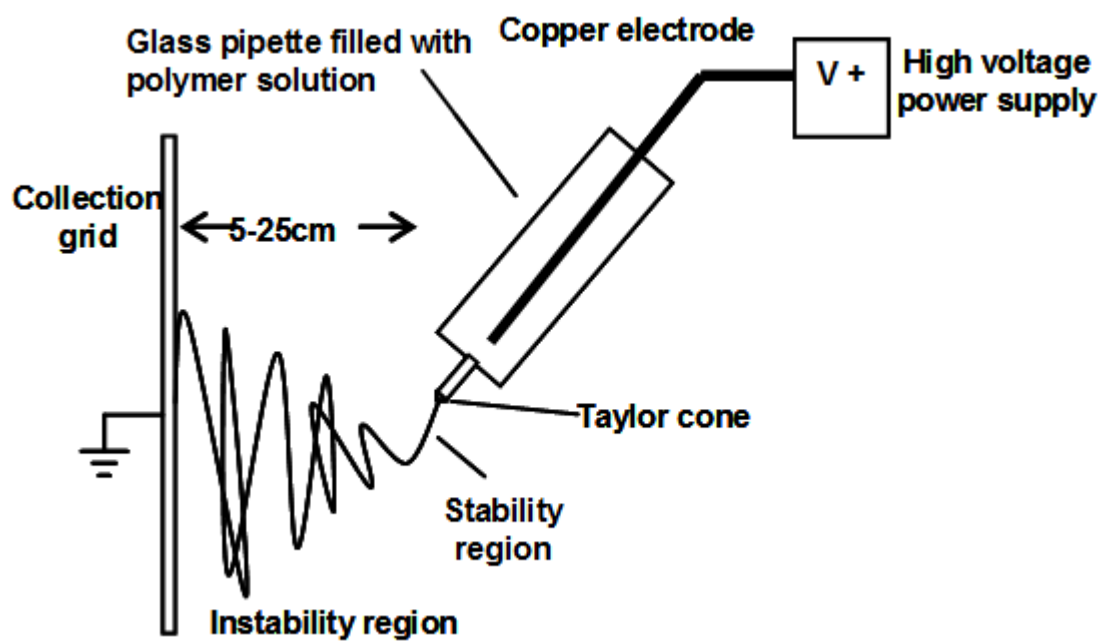
Figure 12. A basic electrospinning setup

3   EXPERIMENTAL

In this chapter, the raw materials used in the electrospinning process, the procedure to prepare the cellulose solutions from kraft pulp, design of experiments and the electrospinning setup are discussed. The details of the different characterization techniques to address the process-structure-property relationships also are provided.

3.1 Materials

4-Methylmorpholine N-oxide solution (50wt% in H_2O, 258822, Sigma) and propyl gallate powder (P3130) were obtained from Sigma Aldrich. Bleached softwood kraft pulp (Pope & Talbot –WRC, DP~1000) was ground to a mesh size of 0.5mm with a Wiley mill. Figure 13 shows the kraft pulp sheet (left) and the kraft pulp in powder form (right).
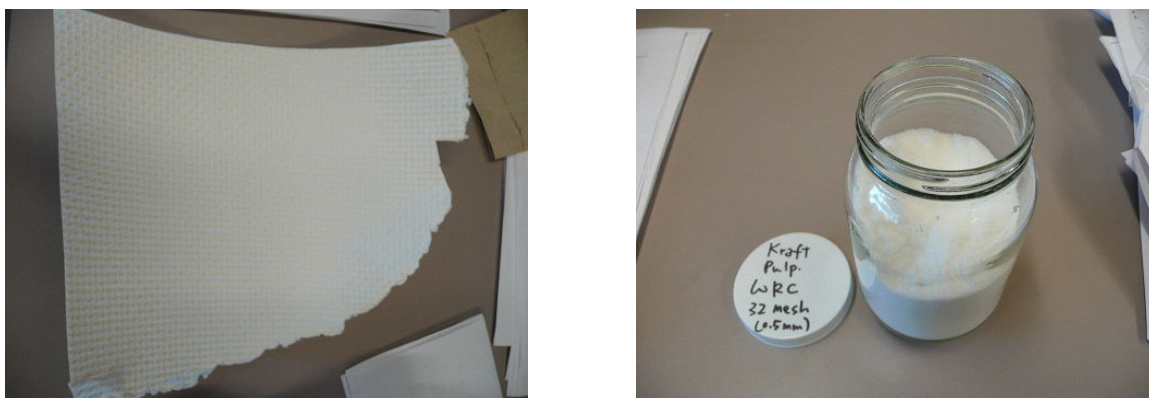
Figure 13. Kraft pulp sheet (left) and ground pulp to 0.5mm mesh size (right)

3.2   Kraft Pulp Dissolution

3.2.1   Solvent Selection

As discussed in Section 2.1, there are several solvent systems for dissolving cellulose. In this study, the NMMO/water solvent system was used to prepare the solution from kraft pulp. The NMMO/water solvent system is the only cellulose solvent system currently used commercially to produce regenerated cellulose fibres in the Lyocell process. The closed-loop process allows up to 99.9% of NMMO to be recovered and recycled, making the NMMO process more environmentally friendly than other solvent systems. While ionic liquids are considered "green" solvents, their high cost prevents them from being used on a commercial scale at present. Kraft pulp dissolution via the DMAc/LiCl solvent system was attempted but was not successful. Undissolved and swollen pulp fibers were observed after the dissolution procedure was completed as described by Kim et al..[90] It appeared that the pulp concentration exceeded the critical dissolution concentration.[91,92] Consequently, the NMMO/water solvent system was chosen over the other cellulose solvent systems.

3.2.2   Solution Preparation

To dissolve kraft pulp completely, the following steps were carried out:[93]

1. Add pulp into a solution containing 50wt%NMMO/ 50wt% water in a flask.

2. Add propyl gallate (anti-oxidant, about 1wt% of pulp) into the mixture.

3. Evaporate the water in the mixture using a RotorVap (Figure 14) under low vacuum (~ -30mmHg) at $80^{o}C$ until a composition of 85wt%NMMO and 15wt% water is obtained. A calculation was done to determine the amount of water that was to be removed to achieve the required composition.

Upon complete dissolution, the resulting solution is a clear brown solution at $80^{o}C$ and a light yellow crystalline solid (Figure 15) at room temperature.

Figure 14. RotoVap (Buchi)

Figure 15. NMMO/water/pulp spinning dope at room temperature

3.2.3 Intrinsic Viscosity Measurement (DP Measurement)

Intrinsic viscosity is the extrapolated value of the reduced viscosity at zero polymer concentration.[94] The purpose of the intrinsic viscosity measurement is to determine the degree of polymerization of a polymer. The degree of polymerization (DP) of kraft pulp and electrospun fibres was measured by determining the intrinsic viscosity by following the procedure described in ISO 5351:2004 (Pulps - Determination of limiting viscosity number in cupri-ethylenediamine (CED) solution). The samples were first conditioned in a controlled environment at $23^{\circ}C$ and 50% relative humidity. 125mg of the sample was dissolved in 50ml of deionized water and 50ml of 1M CED solution. After shaking the solution for 10 minutes to ensure complete and homogeneous dissolution, the solution was placed in the glass viscometer (Solution: Cannon-Fenske, AA482, Size 200; Solvent: Cannon-Fenske, S430, Size 100) that was immersed in a $25^{\circ}C$ water bath. The efflux time (time taken for the liquid meniscus to drop from point A to point B in Figure 16) was measured and used for determining the intrinsic viscosity of the kraft pulp solution.
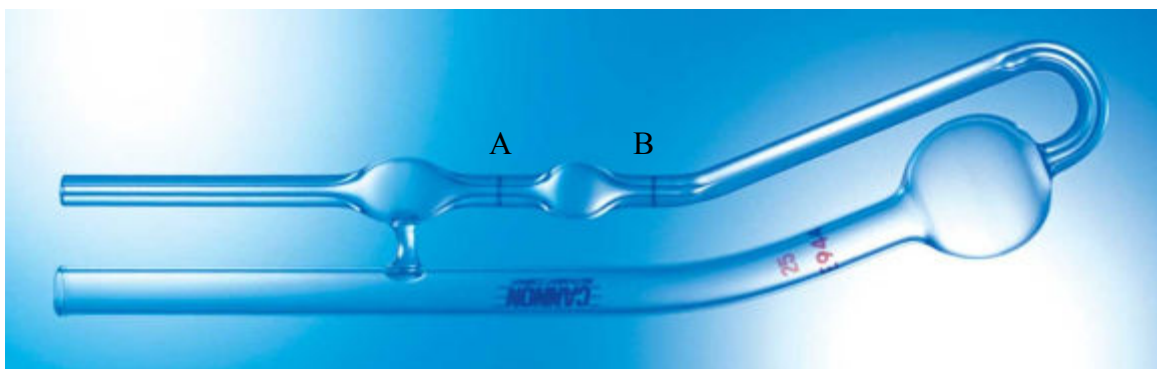
Figure 16. Cannon-Fenske glass viscometer

3.3   Design Of Experiments

To systematically examine the effects of the process parameters on the electrospun cellulose fibre formation and diameter, an experimental design is used. Three process parameters, including polymer solution concentration, nozzle temperature, and voltage, have been identified to be important factors affecting fibre spinnability and fibre diameter.[95] Table 6 is a summary of the process parameters (factors) and the three levels used in the design of experiments.

Table 6. 3-level-3-factor experimental design

Factors	Levels		
	-1	0	+1
Concentration (wt%)	1	2	3
Temperature (^{o}C)	100	120	140
Voltage (kV)	5	7.5	10

Concentration

Preliminary trials showed that 1, 2 and 3 wt% of kraft pulp in NMMO/water (85:15 by weight) would be the optimal range that gives the viscosity to form fibres via electrospinning. 1wt% borders on the lower bound of the concentration because it was observed that electrospraying, instead of electrospinning, occurred at an elevated temperature (140°C) and a medium-level voltage (7.5kV), and only droplets were formed upon coagulation in water bath. Droplet formation due to the electrostatic force is an

indication that the viscosity of the polymer solution is too low for electrospinning to occur. 3wt% appears to be the upper bound of the concentration because it was observed that no fibre formation would occur at a lower temperature (100°C) and a lower voltage (5kV).

Temperature

The kraft pulp/NMMO/water solution is solid at room temperature (20°C) and becomes liquid above 70°C. However, between 70°C and 100°C, the polymer solution is too viscous for electrospinning to occur. Preliminary trials showed that fibre formation would be observed above 100°C. It was reported that the solvent begins to decompose rapidly at a temperature above 150°C and may lead to explosions. Thus for safety reasons, the upper limit of the nozzle temperature was set at 140°C.

Voltage

The voltage supplied induces a potential difference between the nozzle and the target (water surface in this case), which has a fixed distance of 5cm. In previous studies, a voltage range of 0.67 and 4 kV/cm was used to produce electrospun cellulose fibres. [96,97,98] In this study, preliminary trials showed that fibre formation was observed when the voltage ranges from 5kV to 10kV, which is equivalent to 1 and 2 kV/cm, respectively. Above 10kV, the electrospinning process becomes unstable and sparks due to electric arc could be observed.

To investigate the effects of the three factors on fibre formation and diameter, a full factorial experimental design would require a total of $3^3 = 27$ experiments. Preliminary trials with a range of temperature and voltage values showed that 1wt% kraft pulp solution consistently led to film formation instead of fibre formation (Figure 17). Consequently, the design of experiments shown in Table 7 has 18 sets of experiments, instead of 27.
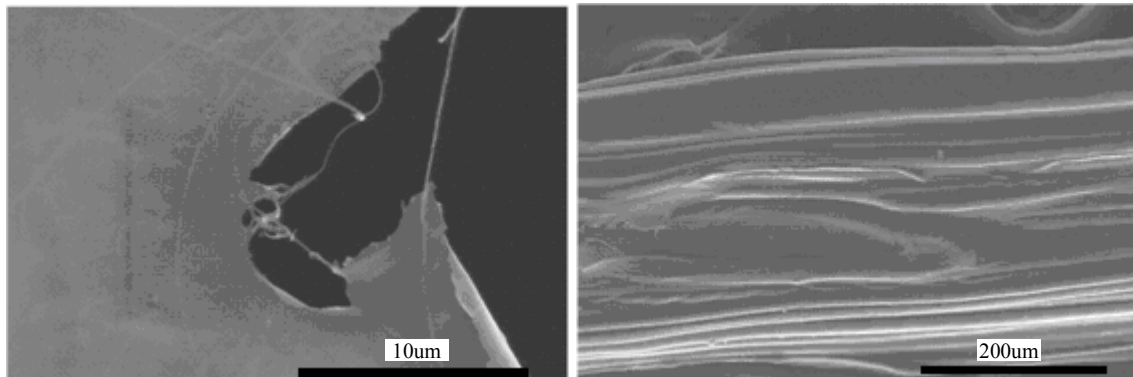
Figure 17. On the left, sample collected from water surface. On the right, samples collected as single fibres and the fibre bundle fused to form a layer of film

Table 7. Design of experiments for electrospun fibres from kraft pulp

Experiment	Conc (wt%)	Temperature (C)	Voltage (kV)
1	2	100	5
2	2	120	7.5
3	2	140	10
4	2	100	7.5
5	2	120	10
6	2	140	5
7	2	100	10
8	2	120	5
9	2	140	7.5
10	3	100	5
11	3	120	7.5
12	3	140	10
13	3	100	7.5
14	3	120	10
15	3	140	5
16	3	100	10
17	3	120	5
18	3	140	7.5

3.4   The Electrospinning Process Of Kraft Pulp-NMMO-Water Solutions

The electrospinning setup (Figure 18) to produce fibres from kraft pulp solutions include a

voltage source, a syringe, an 18.5 G needle (nozzle), a mechanical pump, water bath at

room temperature, a heat jacket and a heat gun. A water bath is required for cellulose

regeneration by coagulation in water. The heat jacket is used to keep the polymer solution

in the syringe at $90^{o}C$ so that the solution remains in liquid state during the electrospinning

process. The heat gun is used to maintain the nozzle temperature at a temperature ranging

from 100 to $140^{o}C$. The solution flow rate is controlled by a mechanical pump at 1mL/hr.

The fibre is either collected as a fibre bundle in the water bath ($20^{o}C$) or in single fibre

form (after coagulation in the water bath) on a rotating drum shown in Figure 18.
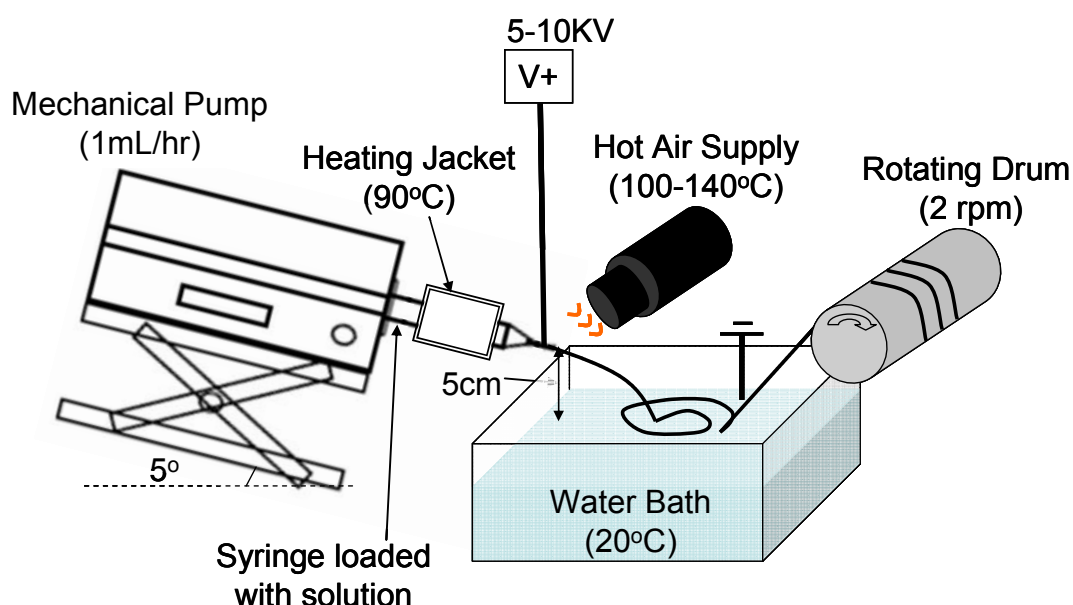
Figure 18. The electrospinning setup to produce electrospun fibres from kraft pulp solutions

Preliminary trials showed that submicron- and micro-fibres could be produced from kraft pulp solutions using the electrospinning process. Consequently, two different fibre collection methods were used for submicron- and micro-fibres, respectively. Submicron-fibres were collected in the form of random fibre bundles, simply because they are too fine to be collected in single fibre form on a rotating drum. Micro-fibres were collected in the form of single fibres on a rotating drum. Figure 19 shows the setup for collecting submicron-fibres in the form of fibre bundles. Because submicron-fibres tend to float and accumulate on the water surface, a vortex is induced to pull the electrospun fibres into the water and thus facilitate fibre coagulation. Figure 20 shows the setup for collecting micro-fibres in the single fibre form using a rotating take-up. Because of the low wet strength of the fibres, it was observed that only fibres with diameters larger than 20um could be collected using this fibre collection method.

Figure 19. Fibre collection for submicron-fibres in random fibre bundles
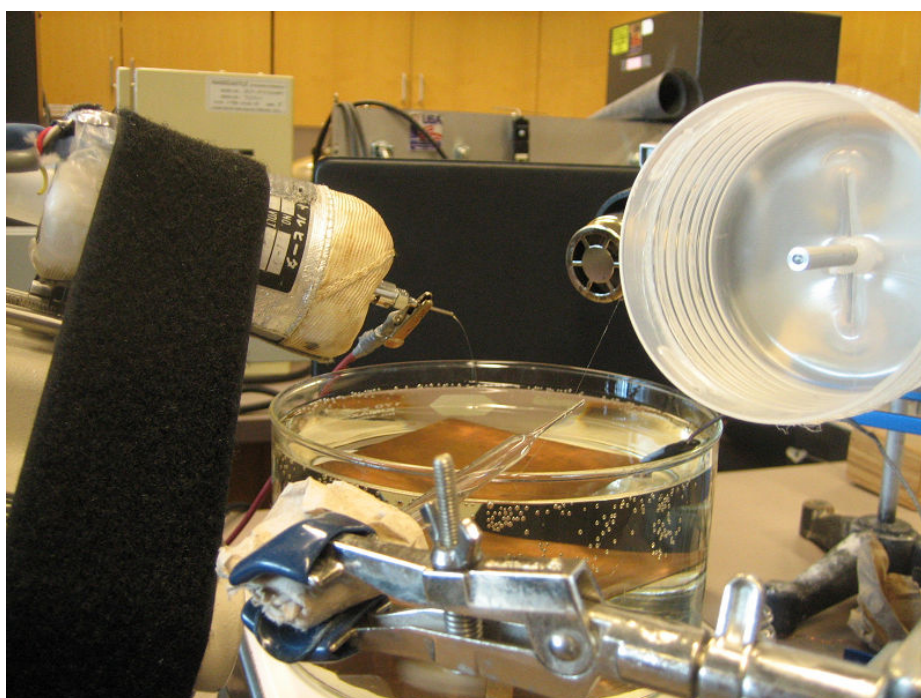
Figure 20. Fibre collection for micro-fibres in single fibre form

3.5   Structural Characterization

3.5.1   Scanning Electron Microscopy (SEM)

Two different scanning electron microscopes were used in this study. Hitachi S2000 SEM was used to examine to general fibre morphology and FEI Quanta FEG 400 Environmental SEM was used to examine the fibre cross section.

To examine the general fibre morphology, the single electrospun fibres and fibre bundles were attached to carbon stickers and then put in an AuPd sputtering chamber for coating to make the samples electrically conductive before SEM observations with the Hitachi S2000.

To observe the fibre cross-section, the electrospun fibres from Experiment #1 were embedded in epoxy resin. After the epoxy resin block was cured, it was microtomed so a clean fibre cross-sectional surface could be obtained for SEM observations. In order to obtain a 3D view of the fibre and its cross-section, the microtomed epoxy resin block was etched to expose a section of the embedded fibres. After etching the epoxy resin block, the block was coated with AuPd in an AuPd sputtering chamber before SEM observations under Quanta FEG 400 Environmental SEM.

3.5.2   Confocal Microscopy

A Zeiss LSM 510 Meta Confocal Microscope was used to examine the cross-sections of the electrospun fibres to obtain the cross-sectional surface area measurement. The electrospun fibres were placed on a glass slide with a thin film of oil for adhesion and covered with a cover slide before being observed under the confocal microscope. Unlike SEM, confocal microscope is a non-destructive method to examine the 3D structure of the fibres using a 3D sectioning technique. The fibre cross-sectional surface areas are measured from the confocal micrographs using the image processing program ImageJ.

3.5.3 Attenuated Total Reflection Infra-red (ATR-IR) Spectroscopy

A Fourier transform infrared spectrometer (FTIR) coupled with the Specac Golden Gate Diamond attenuated total reflection (ATR) optical unit were used to analyze and compare the chemical structure of kraft pulp and different electrospun fibre samples due to the electrospinning process. The analyzed samples were first ground to a mesh size of 0.5mm using a Wiley mill (same sample preparation procedure for TGA, DSC, and contact angle measurements). The spectra were measured with an average of 50 scans and a resolution of 4 cm^{-1}.

3.5.4 X-Ray Diffraction (XRD)

D8 Advance Powder X-ray Diffraction (CuKα, λ=0.154nm) was used for the analysis. The samples were first ground into powder form (using mortar and pestle) and then put in water suspension to be evenly distributed on a zero background plate. After the samples were air-dried, they were analyzed using XRD. The scanning range was 5° to 90° at a scanning rate of 0.02^o/sec.

3.6 Chemical Characterization

3.6.1   Carbohydrate Analysis

After 60-min acid hydrolysis of the sample in 72% sulfuric acid with regular stirring, the mixture was diluted to a 4wt% acid concentration. The diluted mixture was then placed in an autoclave for one hour at $121^{o}C$. After the autoclave cycle, the mixture was allowed to slowly cool to room temperature before unsealing. A set of sugar recovery standards (glucose, xylose, galactose, arabinose, and mannose) was then prepared as described in ASTM E1758-01 "Standard method for the determination of carbohydrate by HPLC". The samples were then analyzed for the respective sugar contents using the High Performance Liquid Chromatography (HPLC).

3.6.2   Energy-dispersive X-ray (EDX) Spectroscopy

Spot analysis using the EDX spectrometer (Quartz XOne system from Quartz Imaging Corp) was conducted on the electrospun fibre to investigate whether there was a difference in elemental composition between the fibre skin and core.

3.7   Physical Characterization

3.7.1   Thermogravimetric Analysis (TGA)

A TA Instrument TGA-Q50 was used for the analysis. Both the electrospun fibres and kraft pulp fibres were ground and then placed in the sample chamber, before the chamber was equilibrated to $25^{o}C$. The temperature was then held at $25^{o}C$ for 1 minute. The chamber was then heated up to $500^{o}C$ at a ramp rate of $10^{o}C/min$.

3.7.2   Differential Scanning Calorimetry (DSC)

Both the electrospun fibres and kraft pulp fibres were ground and the TA Instrument DSC-Q100 was used for the analysis.

Cycle 1: The loading cycle was started by first cooling the sample down to $-40^{o}C$. After holding the temperature at $-40^{o}C$ for 1 minute, the sample was heated to $150^{o}C$ at a ramp rate of $10^{o}C/min$.

Cycle 2: The sample was then cooled down rapidly to $-40^{o}C$ at a ramp rate of $-100^{o}C/min$. The temperature was held at $-40^{o}C$ for 1 minute.

Cycle 3: The sample was heated up to $300^{o}C$ at a ramp rate of $10^{o}C/min$.

3.7.3   Contact Angle Measurements

Both the electrospun fibres and kraft pulp fibres were first ground up. The powder was evenly spread on a 2cm x 2cm double-sided tape such that the tape surface is completely covered. To begin the contact angle measurement, the tip of the hypodermic needle was set at 3.2 mm from the surface of the specimen and a drop of water approximately 1⁄150 to 1⁄200 mL in size was dropped on the specimen. The setup and testing procedure are as described in the ASTM standard D 724 – 99 Standard Test Method for Surface Wettability of Paper (Angle-of-Contact Method).

3.8   Mechanical Characterization

3.8.1   Microtenstile Testing

50 samples of the electrospun single fibres from Experiment 1 with a gauge length of 2cm were mounted on C-shaped frames as shown in Figure 21. A Katotech KES-G1 microtensile tester was used to conduct tensile testing on the 50 samples and to collect the breaking force data. According to ASTM D3822-07, the rate of extension was set at 2mm/min, which is 10% of the initial fibre gauge length. Before the tensile tests, the individual fibre samples were put under an optical microscope to measure the fibre diameters.
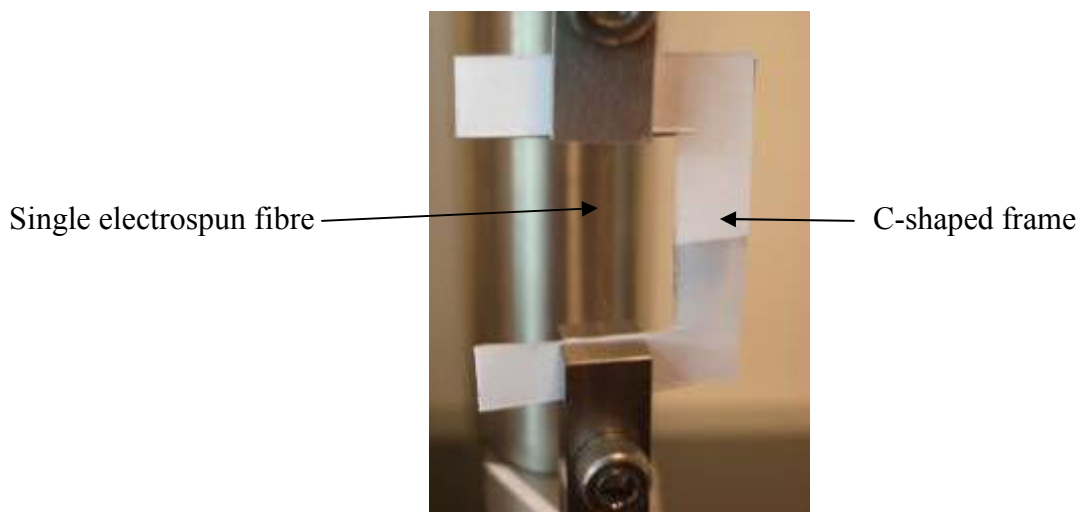
Single electrospun fibre ————⟶   ⟵———— C-shaped frame

Figure 21. An electrospun single fibre with a 2cm gauge length is mounted on a C-shaped paper frame for tensile testing

4 RESULTS AND DISCUSSION

Among the 18 experiments in Table 7, Experiment 1 has been identified as having the optimum electrospinning conditions from the design of experiments, based on the SEM observations. With the current electrospinning setup, only Experiment 1 produced wet fibres that were thick and sufficiently strong to be hand-pulled and subsequently collected on the fibre take-up in continuous single fibre form. The remaining fibre-forming experiments produced wet fibres that were too fine and thus prone to breaking upon hand-pulling following coagulation in the water bath. The only way to collect these fine cellulose fibres was to allow the fibres to accumulate in the water bath and then collect the fibres in an inseparable, entangled fibre bundle form. As a result, only the separable electrospun cellulose single fibres from Experiment 1 (referred to as "electrospun fibres" in the following sections) and the kraft pulp starting material were subjected to the full range of characterization techniques employed in this study, with the exception that SEM was done on fibres from all 18 experiments to observe the general fibre morphology. To demonstrate the reproducibility of the single electrospun fibres, a second run of Experiment 1 was carried out and similar single electrospun fibres were obtained. Characterization was conducted on the single electrospun fibres collected from the first run of Experiment 1. In this chapter, the structure and properties of both the kraft pulp and electrospun fibres based on various characterization results are discussed.

4.1   Intrinsic Viscosity Measurement (DP Measurement)

The solvent system, cellulose concentration, temperature, voltage, and the degree of cellulose polymerization are the predominant factors playing an important role in the cellulose dissolution and electrospinning process. Among these factors, the degree of polymerization is closely related to the fibre formation process and the resulting fibre properties. Carothers and Hills of DuPont stated that the requirements for fibre-forming polymers include having large molecules of more than 12,000g/mol in molecular weight, and the ability of the polymers to crystallize, whereby 3D polymers such as polyamides and polyesters are generally unsuitable.[99] The viscosity of a cellulose solution increases with concentration and molecular weight of the dissolved cellulose. Consequently, when the concentration and molecular weight of the dissolved cellulose reach a critical point, the solution becomes so viscous that electrospinning from the cellulose solution becomes impossible. Generally, the fibre properties including tensile strength, toughness and abrasion resistance are a function of the molecular weight. Therefore accurate cellulose molecular weight measurement is important in determining the cellulose solubility in a particular solvent system, for gauging its fibre-formability, and for understanding the resulting fibre properties.

Intrinsic viscosities of kraft pulp and electrospun cellulose fibres are measured according to ISO 5351:2004 (Pulps - Determination the of limiting viscosity number in cupri-ethylenediamine (CED) solution). Based on the viscosity measurements, the molecular weight and degree of polymerization of both the natural and electrospun fibres were calculated as described below.

Relative viscosity (η_{rel}) is the ratio of the solution viscosity (η) to the solvent viscosity (η_o).

$$\eta_{rel} = \frac{t}{t_o} = \frac{\eta}{\eta_o} \qquad \text{(Equation 4.1.1)}$$

Where

η_{rel} = relative viscosity

t = solution efflux time

t_o = solvent efflux time

η = solution viscosity

η_o = solvent viscosity

Specific viscosity (η_{spec}) is the incremental viscosity due to the presence of the polymer in the solution, where in mathematical expression:

$$\eta_{spec} = \frac{\eta - \eta_o}{\eta_o} = \frac{\eta}{\eta_o} - 1 \qquad \text{(Equation 4.1.2)}$$

The reduced viscosity (η_{red}) is the ratio of the specific viscosity to the polymer concentration (c). This is a measure of the capacity of a polymer to cause the solution viscosity to increase, in other words the incremental viscosity per unit concentration of polymer.

$$\eta_{red} = \frac{\eta_{spec}}{c} \quad \text{(Equation 4.1.3)}$$

By collecting the viscosity measurement data at different cellulose concentrations, the extrapolated value of the reduced viscosity at zero concentration, called intrinsic viscosity [η], can be obtained.

$$[\eta] = \lim_{c \to 0} \frac{\eta_{spec}}{c} \quad \text{(Equation 4.1.4)}$$

The intrinsic viscosity is a unique function of molecular weight and measurement of intrinsic viscosity, and can be used to measure molecular weight by using the Mark-Houwink equation.

$$[\eta] = K \cdot M^{\alpha} \quad \text{(Equation 4.1.5)}$$

Where K and α are constants that vary with polymer, solvent and temperature. M is the average relative molecular mass. For cellulose, K and α are equal to 0.004264 and 1, respectively. The degree of polymerization (DP), the number of repeating units of the polymer chain, can then be computed by dividing the cellulose molecular weight by the

single cellulose repeating unit, which is 161.9 g/mol. It should be noted that the intrinsic viscosity also is affected by the polymer polydispersity. Two polymers with the same molecular weight but different polydispersities have different intrinsic viscosities.

Table 8 and Table 9 summarize the results from the intrinsic viscosity measurements done on kraft pulp and electrospun fibres. Based on these values, the molecular weight and DP of kraft pulp and electrospun fibres were computed and are shown in Table 10, where it can be seen that cellulose molecular chains experience a decrease of approximately 400 in DP during the cellulose dissolution process and the electrospinning process. This result is consistent with the decrease in DP observed in another NMMO-based regenerated cellulose fibre Lyocell, which has a reported DP of 600, as shown in Table 2. Figure 22 and Figure 23 show the interpolation of the reduced viscosity of kraft pulp and electrospun fibres to zero cellulose concentration, which gives their respective intrinsic viscosity.

Table 8. Raw data of the intrinsic viscosity measurements

Sample	Viscometer Constant (cSt/s)	Efflux Time (s)	Solution Kinematic Viscosity (cSt), η	Solvent Kinematic Viscosity (cSt), η_o
CED/Water	0.0147	81.61	-	1.20
Kraft Pulp	0.0954	46.12	4.4	-
Electrospun Fibres	0.0954	28.41	2.7	-

Table 9. Concentration, reduced viscosity, [η].c, and intrinsic viscosity values

Sample	c (g/mL)	η/η_o	[η].c *	[η] (mL/g)
Kraft Pulp	0.0023	3.67	1.633	700.47
Electrospun Fibres	0.0022	2.26	0.948	430.91

*Note: [η].c is the corresponding value of η/η_o obtained from Table 3 of ISO 5351:2004

Table 10. Molecular weight and DP values calculated from intrinsic viscosity measurements

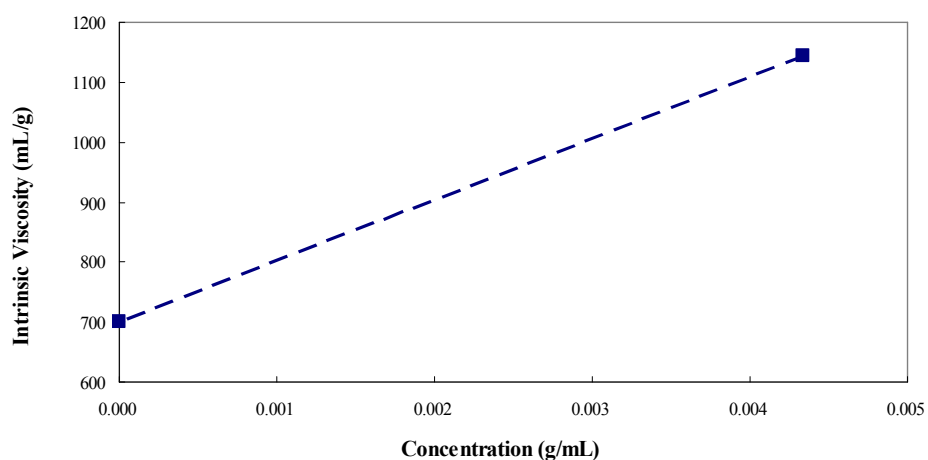| Sample	Molecular Weight	DP
Kraft Pulp	164161	1014
Electrospun Fibres	96708	597

Figure 22. Intrinsic viscosity measurement for kraft pulp
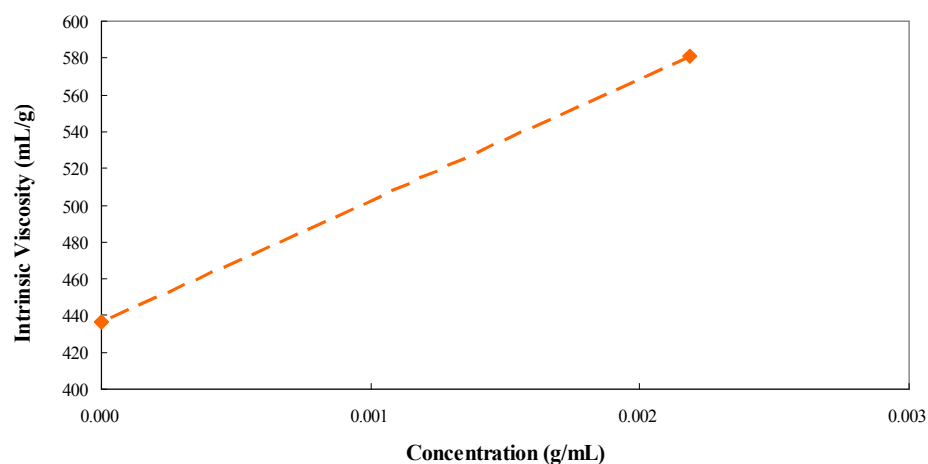

Figure 23. Intrinsic viscosity measurements for electrospun fibres

4.2   Structural Characterization

4.2.1a   Scanning Electron Microscopy (SEM) – General Fibre Morphology

Kraft Pulp

As shown in Figure 24, kraft pulp fibres, like other commercially produced pulp fibres, are not straight and seldom continuous. Kraft pulp fibres contain many defects (dislocations, crimps and kinks in the fibre cell wall) along their length. Deformations typically fall into two categories: (1) natural deformities in the living trees, such as pits, or (2) induced through deliberate or incidental mechanical impact during processing. Induced deformations are primarily caused by axial compressive failure of the wall during pulp processing, which generally leads to structural changes in the fibre body and in the ultrastructure of the fibres. They do not allow the fibres' strength potential to be fully realized, and thus limit the applications of pulp fibres in making load-bearing products at a wide range of environmental conditions. Re-engineering and custom-designing cellulose fibres to make them more moisture-resistant and mechanically stronger are necessary first steps towards developing high value-added products, from a completely renewable resource, for advanced applications in electronic printing, packaging and in structural materials for the automotive and aerospace industries.
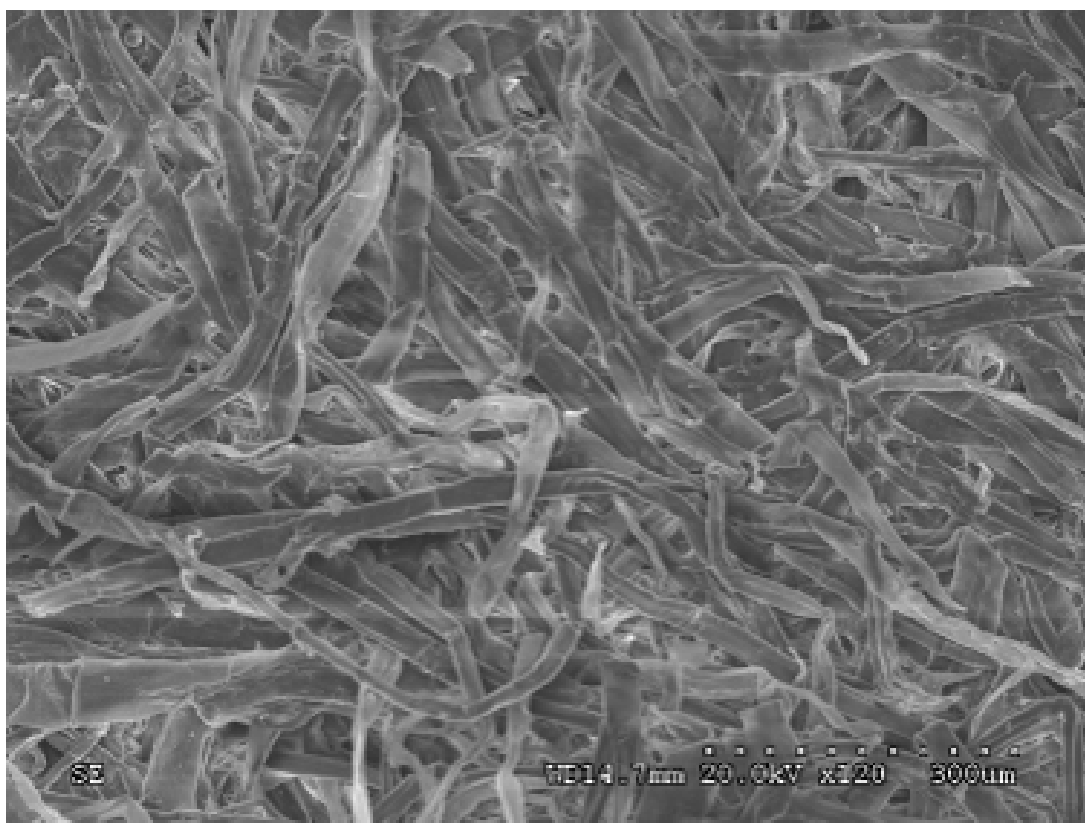
Figure 24. SEM of kraft pulp

Electrospun cellulose fibres from 1wt% kraft pulp solution

As discussed in Section 3.3, Figure 17 shows the SEM of samples from preliminary trials (using various electrospinning conditions) collected both from water surface in the form of a film and as single fibres, which would fuse together to form a film. These res could be due to the presence of solvent in the fibres coagulated in water bath that causes the fibres in contact with each other to fuse together and form a film. The 99wt% of solvent in the polymer solution appears to be too high for effective solvent removal in the water bath and consequent fibre separation after water coagulation.

Electrospun cellulose fibres from 2wt% kraft pulp solution

Figure 25 shows the electrospun fibres from 2wt% kraft pulp solutions. The SEM image shows that submicro- and micro-fibres can be electrospun from the 2wt% kraft pulp solutions. Electrospun micro-fibres with an average fibre diameter of 25.2μm were collected in single fibre form. Smaller fibres, including those on a submicron scale, were collected in the form of random fibre bundles.

Electrospun cellulose fibres from 3wt% kraft pulp solution

Figure 26 shows the electrospun fibres from 3wt% kraft pulp solutions. At 5kV, no fibres could be produced. No electrospinning jet was observed at the tip of the spinneret at a voltage 5kV for the 3wt% solutions, suggesting that the electrostatic forces due to the electric field were smaller than the solution surface tension.
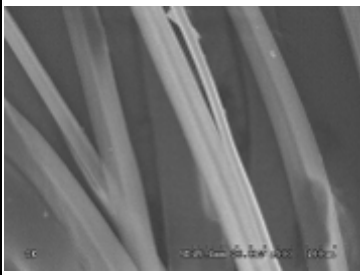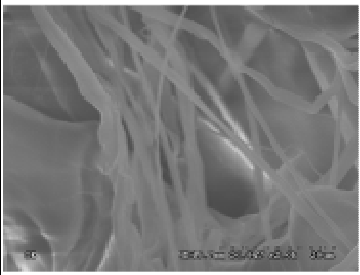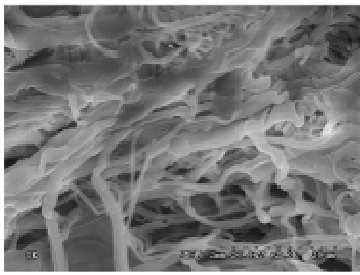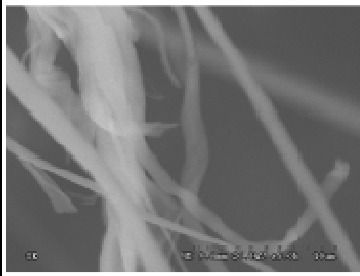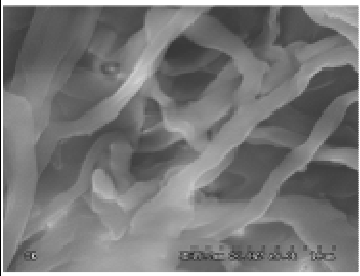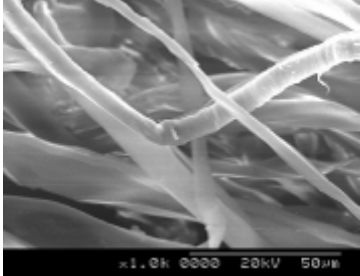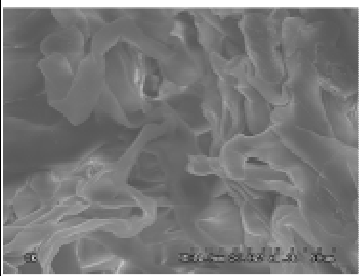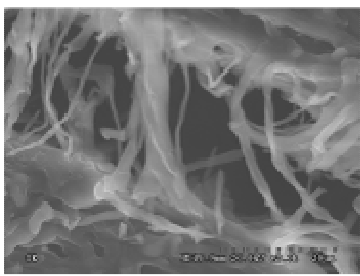
EXP 1 (500X)	EXP 4 (2000X)	EXP 7 (2000X)
AVE DIA: 25.2±11.9 μm MIN/MAX: 4.5 / 56.9 μm	AVE DIA: 1.3±0.7 μm MIN/MAX: 0.3 / 3.3 μm	AVE DIA: 1.1±0.5 μm MIN/MAX: 0.4 / 2.6 μm
EXP 2 (5000X)	EXP 5 (5000X)	EXP 8 (1000X)
AVE DIA: 0.9±0.4 μm MIN/MAX: 0.4 / 0.8 μm	AVE DIA: 2.1±0.9 μm MIN/MAX: 1.0 / 4.6 μm	AVE DIA: 13.5±6.9 μm MIN/MAX: 9.6 / 22.2 μm
EXP 3 (1000X)	EXP 6 (1000X)	EXP 9 (2000X)
AVE DIA: 2.8±1.4 μm MIN/MAX: 0.7 / 5.9 μm	AVE DIA: 7.6±3.7 μm MIN/MAX: 2.0 / 21.0 μm	AVE DIA: 1.1±0.4 μm MIN/MAX: 0.6 / 2.1 μm

Figure 25. Electrospun fibres from 2wt% kraft pulp solutions
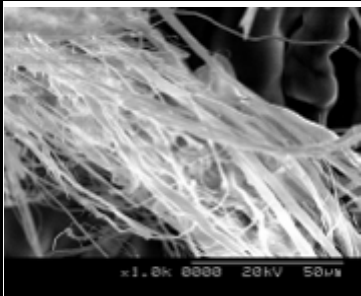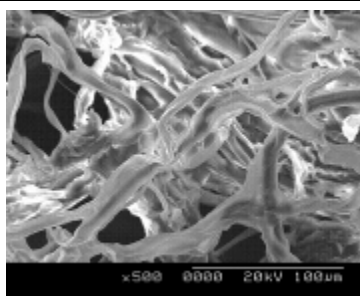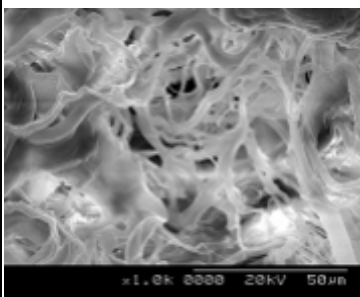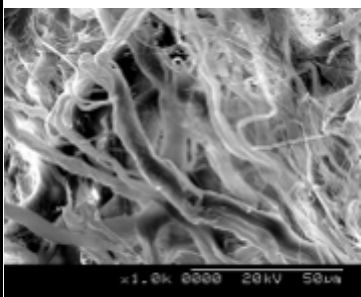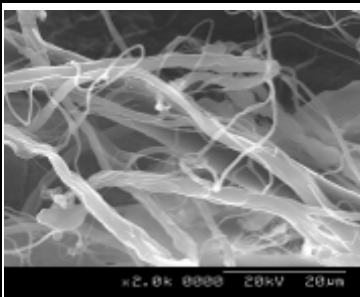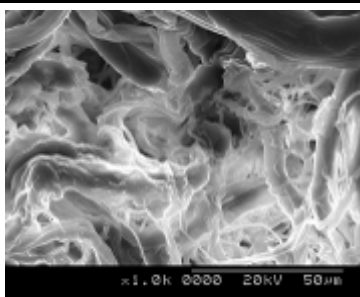
EXP 10	EXP 13 (1000X)	EXP 16 (500X)
NO FIBRE		
	AVE DIA: 1.6±0.9 µm MIN/MAX: 0.5 / 4.0 µm	AVE DIA: 7.8±4.0 µm MIN/MAX: 2.2 / 17.2 µm
EXP 11 (1000X)	EXP 14 (5000X)	EXP 17 (1000X)
		NO FIBRE
AVE DIA: 5.9±4.6 µm MIN/MAX: 1.4 / 19.2 µm	AVE DIA: 3.0±1.9 µm MIN/MAX: 0.3 / 8.7 µm	
EXP 12 (2000X)	EXP 15	EXP 18 (1000X)
	NO FIBRE	
AVE DIA: 4.7±3.1 µm MIN/MAX: 1.5 / 18.7 µm		AVE DIA: 3.2±3.0 µm MIN/MAX: 0.7 / 16.0 µm

Figure 26. Electrospun fibres from 3wt% kraft pulp solutions

Table 11. Electrospun cellulose fibre diameters

Exp	Conc (wt%)	Temp (C)	Voltage (kV)	Fibre Diameter (μm)	Standard Dev (μm)	Coefficient of Variation
1	2	100	5	25.2	11.9	47%
2	2	120	7.5	0.9	0.4	48%
3	2	140	10	2.8	1.4	49%
4	2	100	7.5	1.3	0.7	54%
5	2	120	10	2.1	0.9	46%
6	2	140	5	7.6	3.7	49%
7	2	100	10	1.1	0.5	51%
8	2	120	5	13.5	6.9	51%
9	2	140	7.5	1.1	0.4	32%
10	3	100	5	n/a	n/a	n/a
11	3	120	7.5	5.9	4.6	77%
12	3	140	10	4.7	3.1	66%
13	3	100	7.5	1.6	0.9	57%
14	3	120	10	3.0	1.9	63%
15	3	140	5	n/a	n/a	n/a
16	3	100	10	7.8	4.0	51%
17	3	120	5	n/a	n/a	n/a
18	3	140	7.5	3.2	3.0	92%

Diameters of electrospun cellulose fibres from 2wt% kraft pulp solution

Diameter measurements were carried out on 40 different electrospun fibres from each experiment using the scanning electron micrographs. From Table 11, the average electrospun fibre diameter from 2wt% solutions ranges from 0.9 to 25.2μm. This shows that submicron and micro-fibres could be produced using the electrospinning process by varying the process parameters. The coefficient of variation of the 2wt% average fibre diameter has an average of 48%, which is significantly lower compared to that of the 3wt% fibres at 73%. This further suggests that 2wt% is the optimum concentration to produce cellulose fibres via electrospinning.

Diameters of electrospun cellulose fibres from 3wt% kraft pulp solution

Diameter measurements were carried out on 40 different electrospun fibres from each experiment using the scanning electron micrographs. From Table 11, the average electrospun fibre diameter from 3wt% solutions ranges from 1.6 to 7.8μm. As discussed above, the average fibre diameter from 3wt% kraft pulp solution has a significantly higher coefficient of variation. This could be attributed to the higher viscosity of the 3wt% solution which caused difficulty in forming a stable electrospinning jet.

Concentration effect on spinnability and fibre diameter

The solution spinnability was observed to decrease with increasing concentration. At 1wt% cellulose concentration, the solution was observed to be spinnable. However, as shown in Figure 17, no fibres could be collected because the electrospun fibres fused together to form a film structure. From 2wt% to 3wt%, it was observed that the spinnability decreases. While the 2wt% solutions could be electrospun at a voltage of 5kV, the 3wt% solutions produced no fibres at the same voltage, indicating a decrease in solution spinnability at 3wt%. As the cellulose concentration increases, the electrospun fibre diameter increases as shown in Figure 27. An increase in cellulose concentration leads to an increase in solution viscosity[100], resulting in lower solution spinnability and a smaller extent of fibre elongation during the electrospinning process, and thus larger fibre diameters.
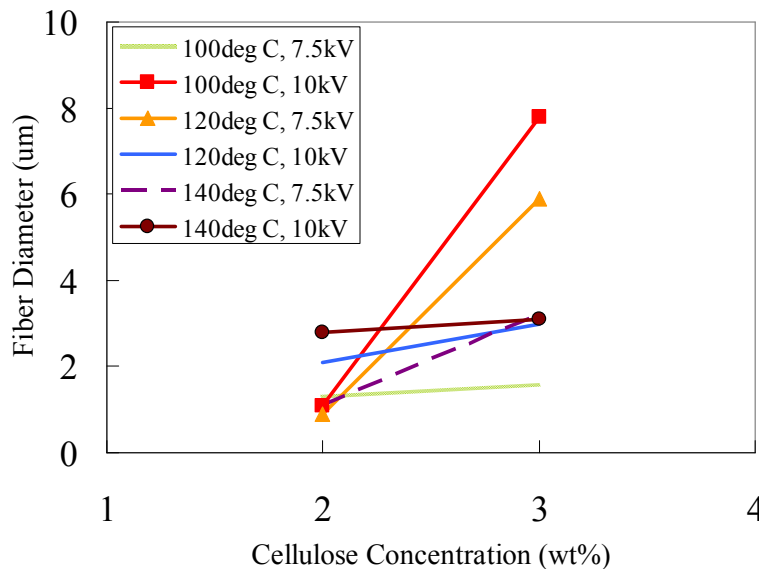
Figure 27. Concentration effect on fiber diameter

Temperature effect on spinnability and fibre diameter

As temperature increases, the solution viscosity decreases due to molecular chain relaxation[101]. A lower solution viscosity results in a higher spinnability because smaller electrostatic forces are required to over the surface tension of the solution at a higher temperature. As shown in Figure 28, the fibre diameter decreases with increasing temperature at 2wt% and 5kV, suggesting that the solution experienced a greater extent of elongation during the electrospinning process at higher temperatures. However, for medium (7.5kV) and high (10kV) voltage levels using 2wt% solutions, the air temperature does not appear to have a significant effect on the fibre diameter.
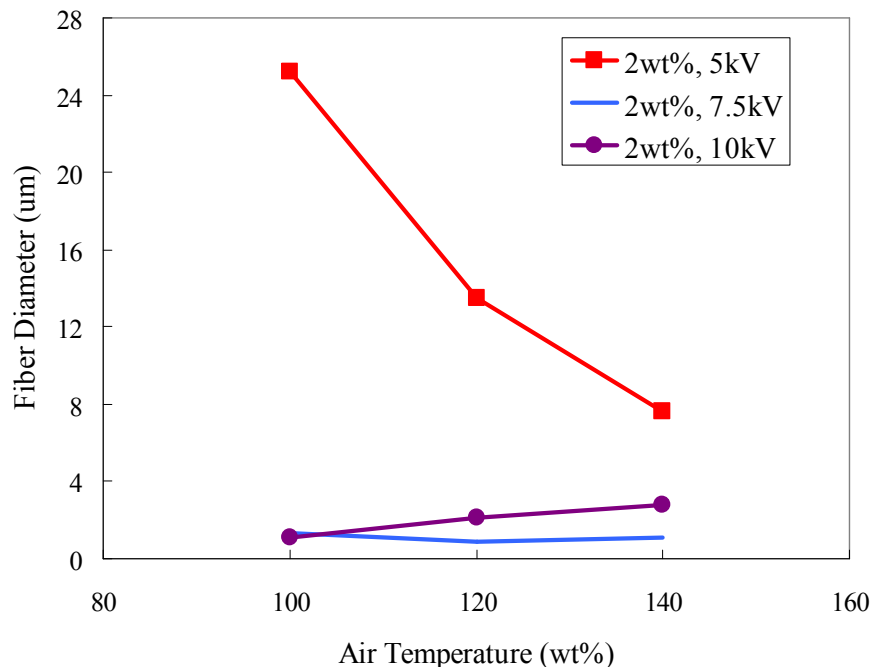
Figure 28. Temperature effect on electrospun fibre diameter

Voltage effect on spinnability and fibre diameter

As voltage increases, the electrostatic forces increase and the potential difference between the spinneret and the ground increases. Higher electrostatic forces imply a greater ease in overcoming the surface tension of the solution. Consequently, the solution spinnability increases with increasing voltage. Higher electrostatic forces would lead to a greater extent of elongation during the electrospinning process, resulting in a smaller fibre diameter. As shown in Figure 29, fibre diameter consistently decreases from 5kV to 7.5kV at 100, 120 and 140°C, and does not appear to vary significantly from 7.5kV to 10kV. The voltage appears to have a significant effect on the fibre diameter when increasing the voltage from the low (5kV) level to the medium (7.5kV) level. No significant voltage effect on the fibre diameter was observed when increasing the voltage from the medium level (7.5kV) to the high level (10kV).
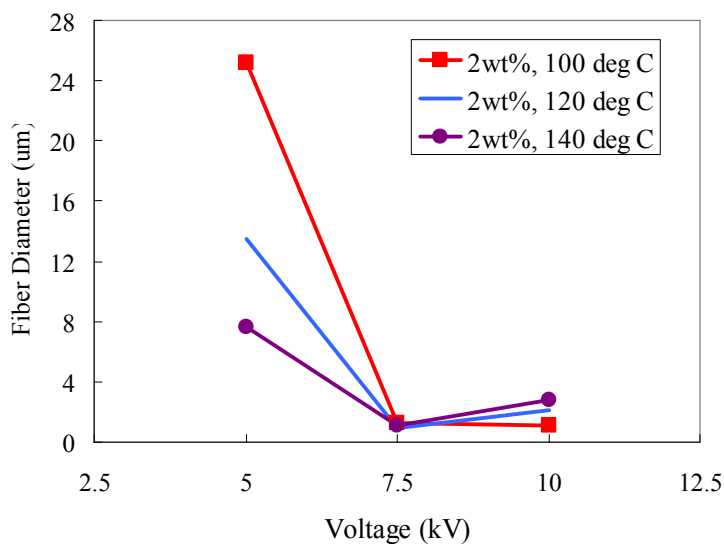
Figure 29. Voltage effect on electrospun fibre diameter

Response Surface Analysis of voltage and temperature effects on fiber diameter

Using DesignExpert, the Response Surface Analysis of the voltage and temperature effects on the average fiber diameter from the 2wt% cellulose solutions was examined, based on the data in Table 11. Based on the Response Surface Analysis (Figure 30), to obtain electrospun fibres with a 0.1um average fibre diameter, the electrospinning conditions are 2wt% cellulose solution, 8.8kV of voltage and 100°C. However, due to the large coefficients of variance in the average fibre diameters shown in Table 11, Experiments 1 to 9 should be repeated to show reproducibility of the fibre diameter data and, subsequently, improve the reliability of the Surface Response Analysis shown below.
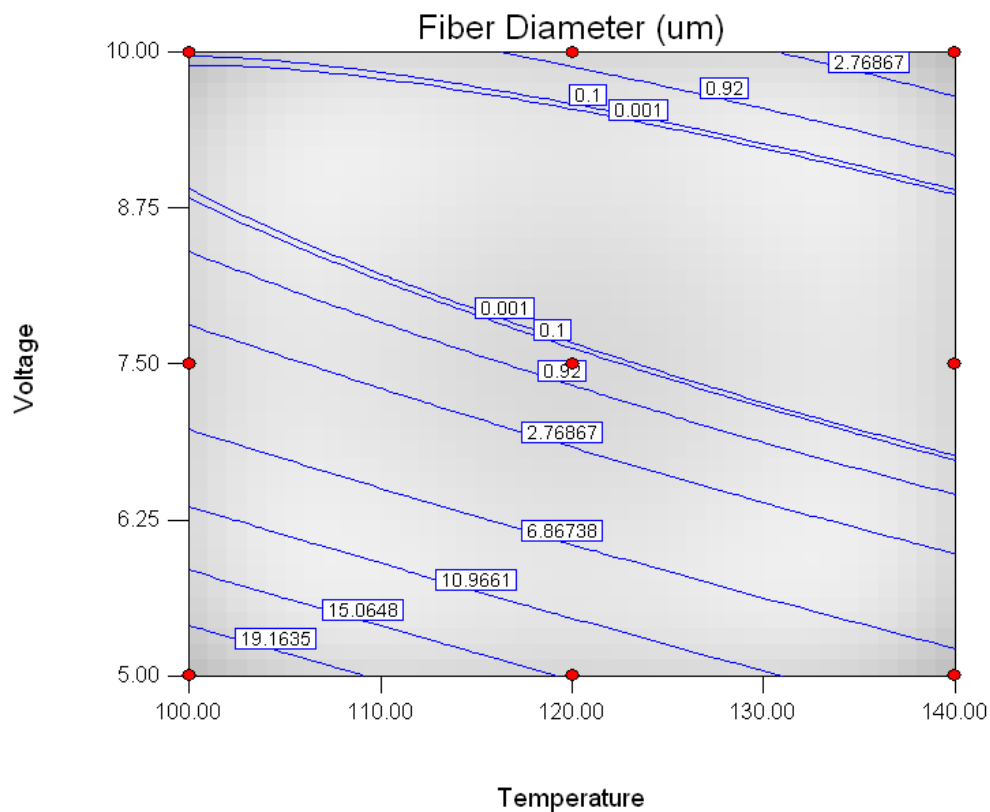
Figure 30. Response Surface Analysis of the electrospun fibre diameter

4.2.1b   Scanning Electron Microscopy (SEM) – Fibre Cross Section

To further examine the fibre morphology, the electrospun fibres from Experiment 1 were microtomed to obtain a clean fibre cross-sectional surface for observation under SEM. Figure 31 shows that the electrospun fibres appear to have irregular shapes with a skin-core microstructure, which has also been observed in other solvent-spun regenerated cellulose fibres, including Viscose and Lyocell.[102] The irregular and varying shapes of the fibre cross section suggest that the electrospinning processing parameters need to be further optimized so that fibres with a consistent and reproducible shape can be obtained. Viscose fibres have a skin–core structure with 25-150 nm voids in the core region and a densified 1.5–2.5 μm skin layer with 5–25 nm pores. The skin thickness of the electrospun fibres was measured to be approximately 100nm. The skin-core microstructure of the electrospun fibres suggests that the fibres could have experienced a two-stage precipitation during coagulation in the water bath, in which the skin precipitates faster than the core and thus has a different microstructure from the core. [103] However, it is not immediately clear whether the skin structure was formed during the coagulation process or during the drying process, when the skin wrinkles due to the significant reduction in size of the fibre core. It is important to recognize the presence of the skin-core microstructure because regenerated cellulose fibres with a skin-core structure are inferior in mechanical properties to homogeneous fibres.[104]
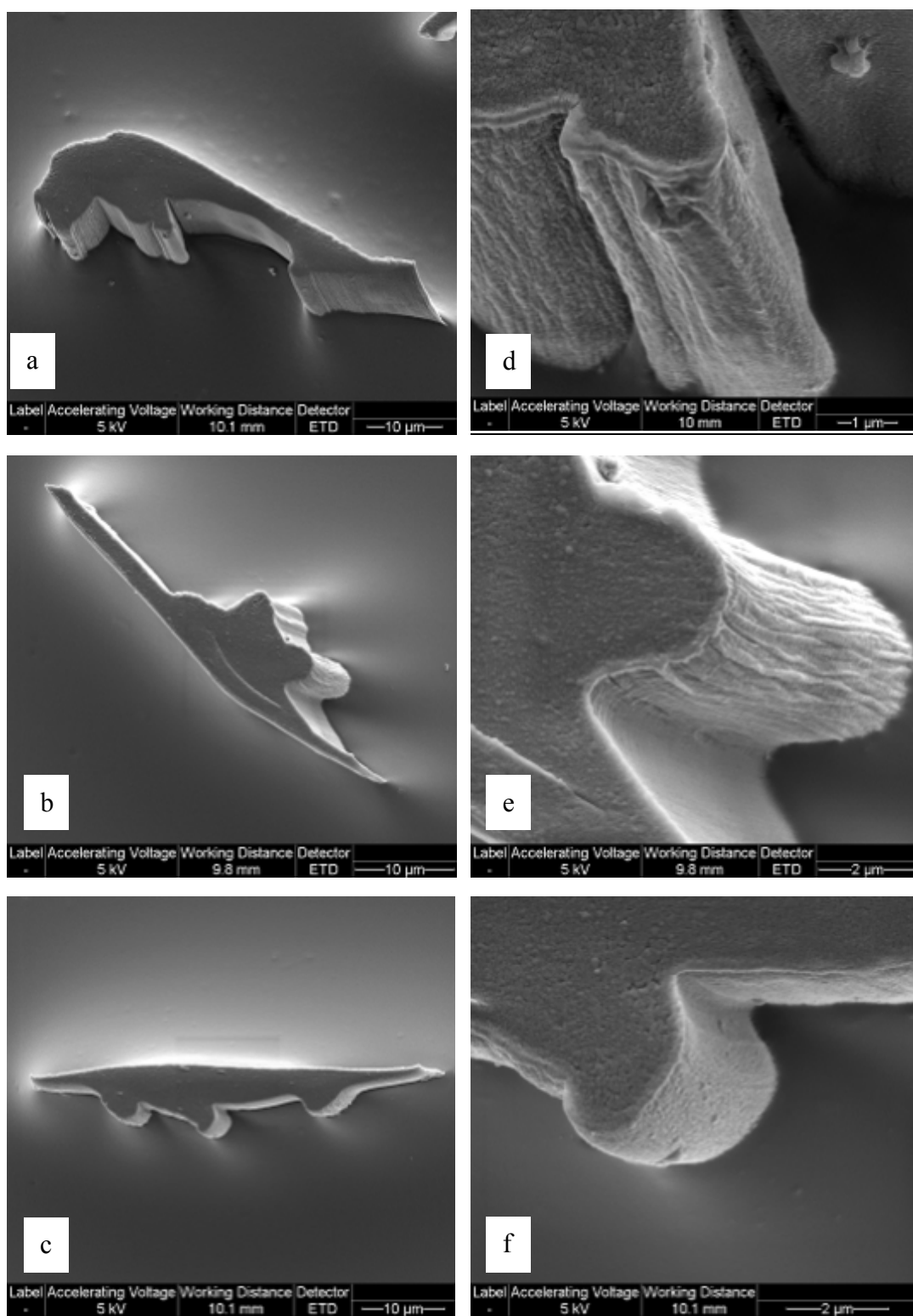
Figure 31. SEM images on the right (d,e,f) are the respective enlarged sections of the SEM images on the left (a,b,c), showing the electrospun fibre skin-core microstructure

Fibrillation-free Electrospun Cellulose Fibres

In contrast to viscose and Lyocell (Figure 32), fibrillation, which is detrimental to the fibre mechanical performance, is not observed in the electrospun fibres. The non-fibrillated microstructure indicates that there is a potential to produce high-quality regenerated cellulose fibres by electrospinning from kraft pulp.
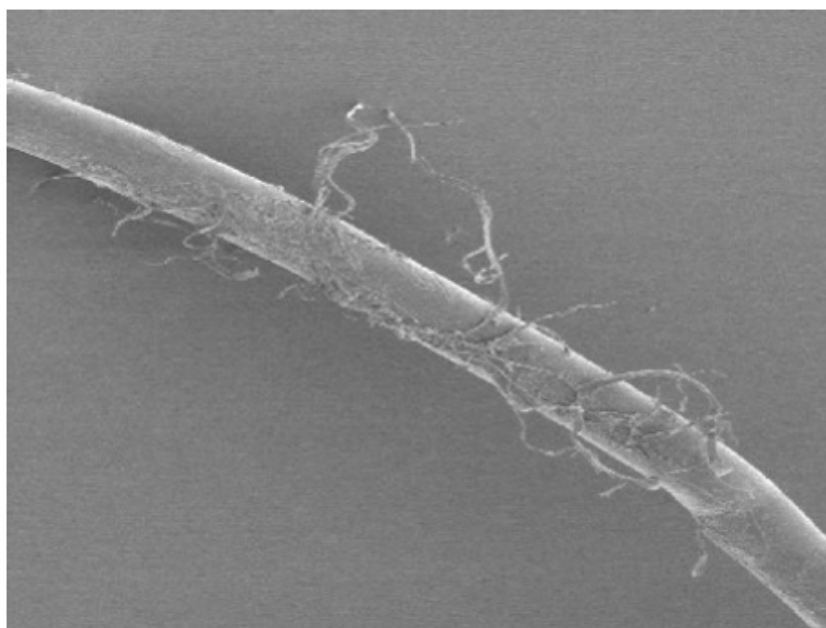
Figure 32. Micrograph showing fibrillation of a single Lyocell fibre [64]

Nano-filament structure of the electrospun cellulose fibre

Figure 33 (SEM) and Figure 34 (illustration) show that the electrospun cellulose fibre has a nano-filament structure with diameters averaging 80-120nm. A more accurate measurement of the nanao-filament diameter will have to be carried out using transmission electron microscopy. In addition to the fibrillation-free microstructure, the

nano-filament structure is another indication that high-strength cellulose fibres can potentially be produced using the electrospinning process.

Label	Accelerating Voltage	Working Distance	
-	5 kV	10.1 mm	�╾2 µm╼
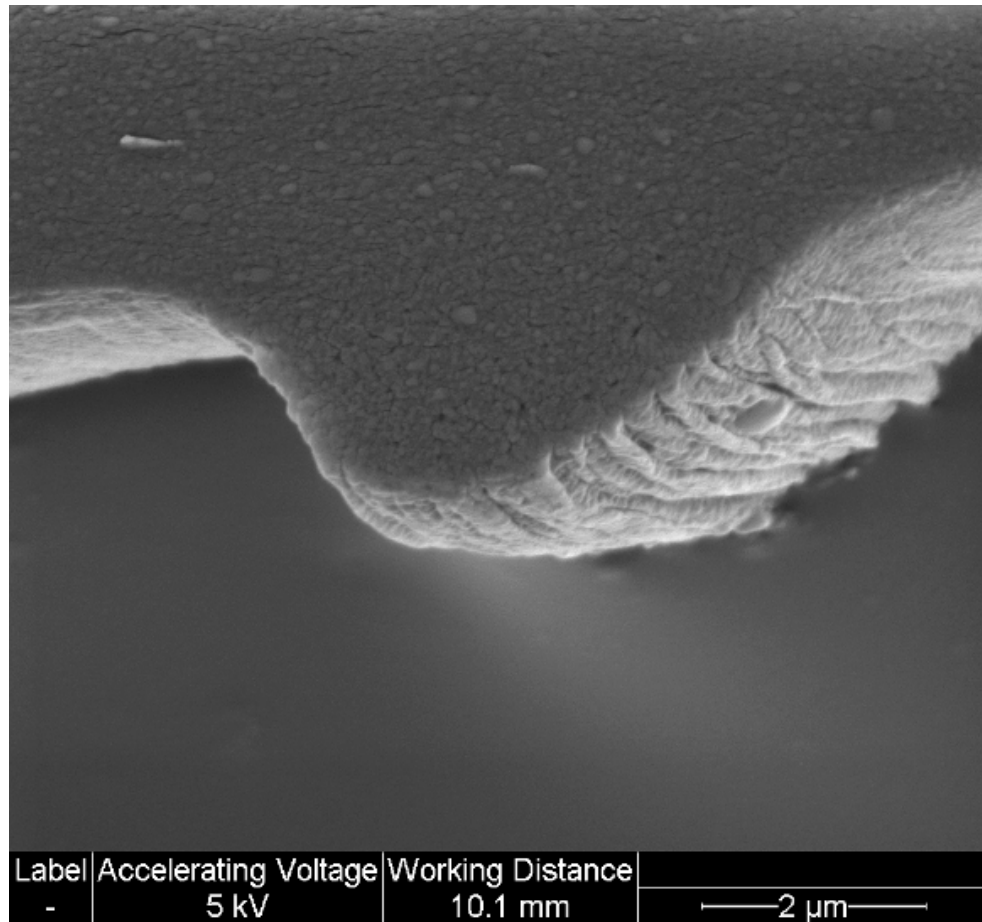
Figure 33. SEM (30000x) showing the nano-filament structure of the electrospun fibre
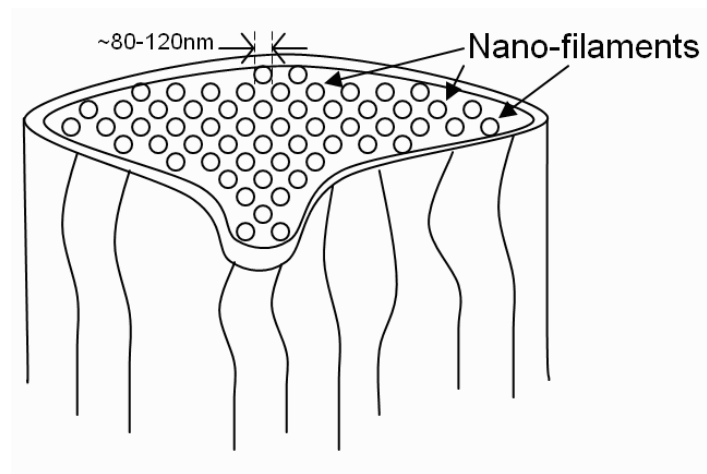
Figure 34. Illustration showing the nano-filament structure of an electrospun fibre

4.2.2 Confocal Microscopy

It can be seen from Figure 31 that the electrospun fibres from Experiment 1 do not have a regular cross-sectional shape. Furthermore, the variance in the fibre cross-sectional surface areas is not known. To accurately determine the mechanical properties, the fibre cross-sectional surface area must be accurately measured. In this study, the 3D sectioning technique available in confocal microscopy is used for the purpose of accurately measuring the fibre cross-sectional surface area. The confocal micrographs in Figure 35 show the cross-section of four different electrospun single fibres. The irregular, varying fibre cross-sectional shapes are consistent with the observation from SEM. The distribution of the fibre cross-sectional surface area from 40 fibres is shown in Figure 36. Cross-sectional surface area measurements of the 40 samples using ImageJ gave an average cross-sectional area of $117\pm50\mu m^2$, indicating that the electrospun fibres have a significant variability in both the cross-sectional shape and surface area.
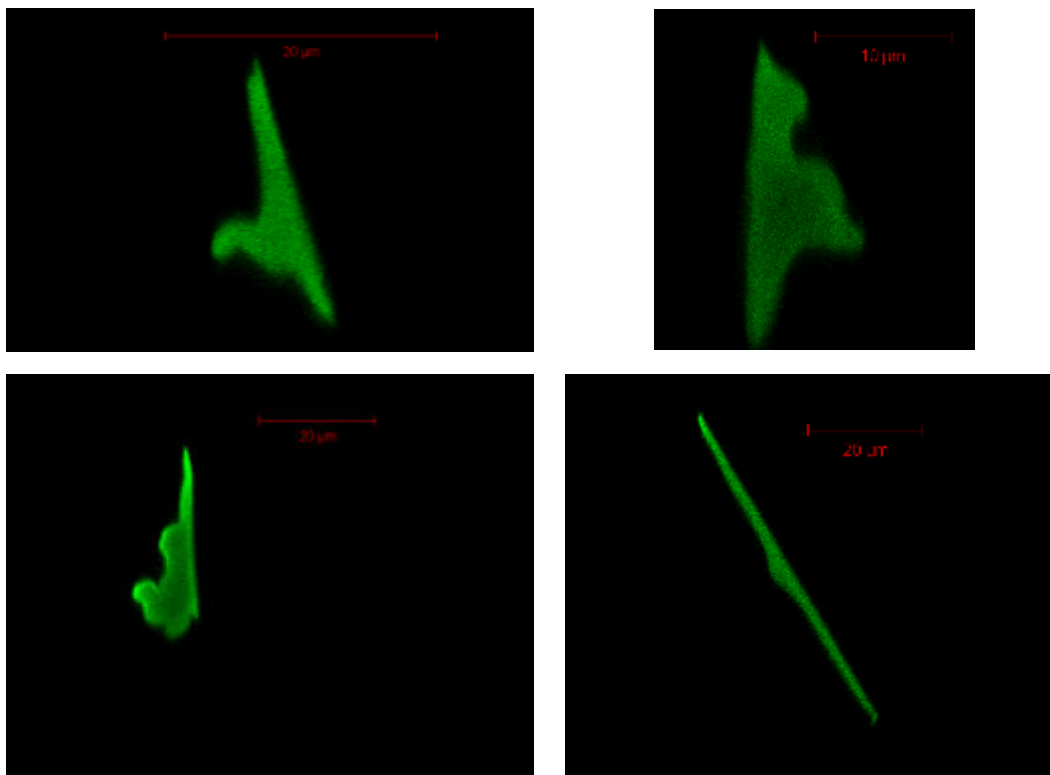
Figure 35. Confocal micrographs of the electrospun fibre showing the fibre cross-sectional surface
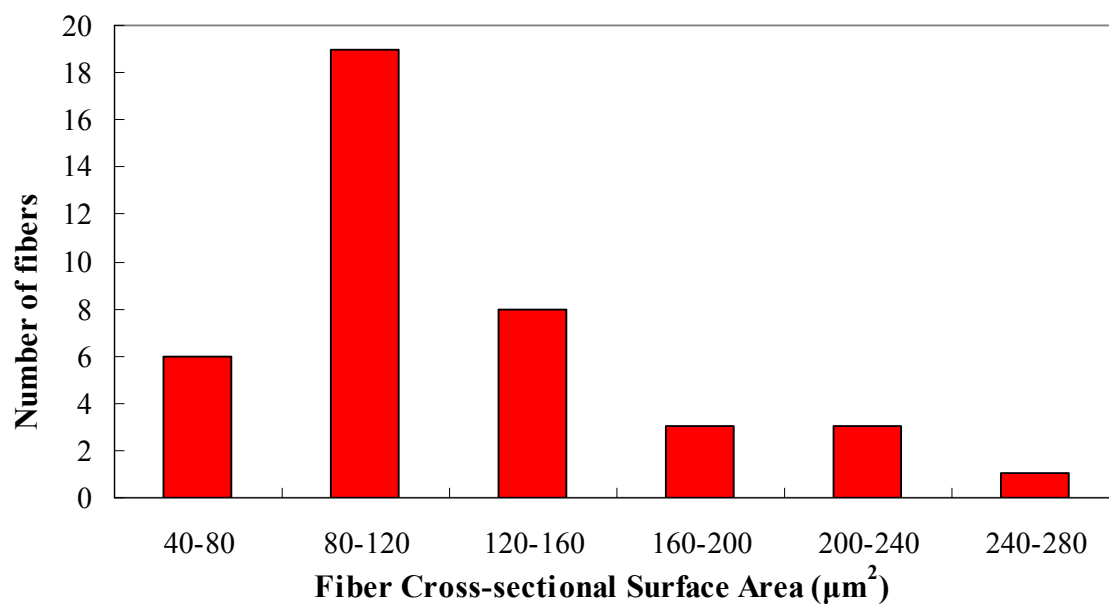
Figure 36. Histogram of the electrospun fibre cross-sectional surface area

4.2.3   Attenuated Total Reflection Infra-red (ATR-IR) Spectroscopy

In Figure 37, the band at 1155cm^{-1} is ascribed to the asymmetric bridge C-O-C stretching in cellulose and hemicellulose. The 893cm^{-1} band is characteristic of the group C_1 frequency in cellulose. The band at 1045-1055cm^{-1} corresponds to the C-O stretch. Since there is no new peak observed in the IR spectrum of the electrospun fibres, cellulose in the electrospun fibres most likely was not derivitized and the cellulose chemical structure was largely preserved during the cellulose dissolution process and the electrospinning process (Figure 37).[105] However, the 1455cm^{-1} band, which corresponds to the –OH in-plane bending of electrospun cellulose fibres appears to become less prominent. This suggests that (1) there is bridging of the hydroxyl groups between the inter-molecular chains in the electrospun fibres, or (2) the hydroxyl groups of cellulose appear to have been diminished in electrospun fibers compared to kraft pulp, indicating that the cellulose rink environment has changed, which would be consistent with the observed decreased hydrophilicity. However, Raman spectroscopy studies would be needed to further explore this hypothesis. The IR hydroxyl group stretching region in the vicinity of 3000cm^{-1} should be investigated in future work for confirmation. In Section 4.4.3, the contact angle measurements show that the electrospun fibers in fact do appear to be more hydrophobic than kraft pulp. Table 12 shows the assignments of the most significant IR bands in crystalline cellulose I and II as reported in previous published results.[106,107,108]
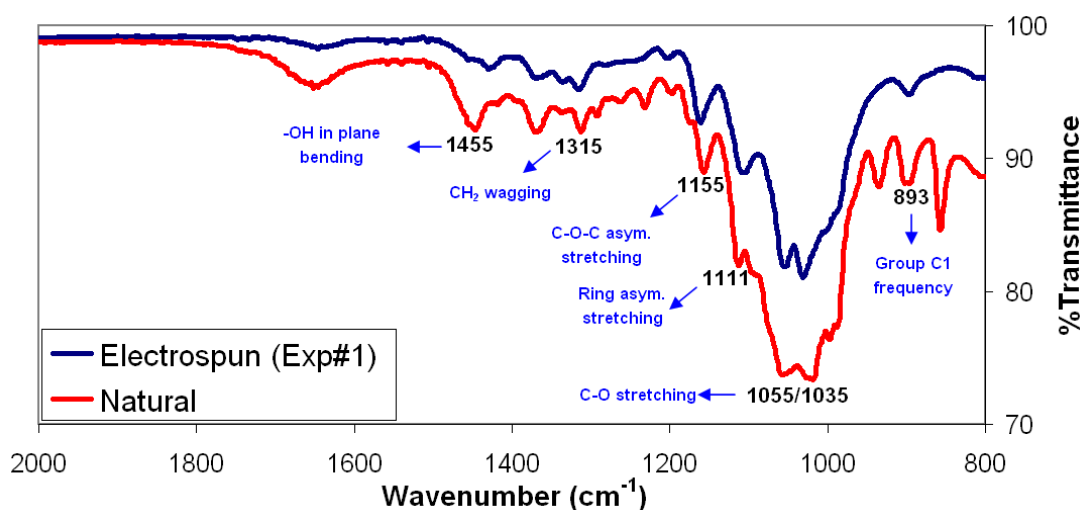
Figure 37. ATR-IR spectra of electrospun versus kraft pulp fibres

Table 12. Characteristic frequencies from the infrared spectra in crystalline polysaccharide [106-108]

Frequency (cm^{-1})	Assignment	Component
3488	–OH stretching intramolecular hydrogen bonds	Cellulose II
3447	–OH stretching intramolecular hydrogen bonds	Cellulose II
3405	–OH stretching intramolecular hydrogen bonds	Cellulose I
3350	–OH stretching intramolecular hydrogen bonds	Cellulose I and Cel II
3175	–OH stretching intramolecular hydrogen bonds	Cellulose II
2970	CH stretching	Cellulose I and Cel II
2945	CH stretching	Cel I(2945) Cel II(2955)
2900	CH stretching	Cellulose I and Cel II
2853	CH$_2$ asymmetric stretching	Cellulose I and Cel II
1635	OH of water absorbed from cellulose	Cel I(1430) Cel II(1420)
1455	–OH in plane bending	Cel I(1455) Cel II(1470)
1420	CH$_2$ symmetric bending	Cel I and Cel II
1375	CH bending	Cellulose I and Cel II
1335	–OH in plane bending	Cel I(1336) Cel II(1335)
1315	CH$_2$ wagging	Cel I(1317) Cel II(1315)
1278	CH bending	Cel I(1282) Cel II(1278)
1200	–OH in plane bending	Cel I(1205) Cel II(1200)
1155	C–O–C asymmetric stretching	Cel I(1155) Cel II(1162)
1111	Ring asymmetric stretching	Cel I(1111) Cel II(1007)
1055	C–O stretching	Cellulose I and Cel II
1035	stretching C–O	Cellulose I and Cel II
893	Group C$_1$ frequency	Cel I(895) Cel II (893)

4.2.4   X-Ray Diffraction (XRD)

XRD analysis was conducted on electrospun single fibres from kraft pulp and raw kraft pulp fibres to examine the crystal structure. The XRD pattern of electrospun fibres show broader peaks compared to kraft pulp, indicating that there is less crystalline region in the electrospun fibres. Raw pulp fibres have the crystal structure of cellulose I (native cellulose), as shown in Figure 38.[109] Electrospun fibres appear to have a similar crystal structure of cellulose I with a shift in the peaks of 2.3°. The ability to produce electrospun cellulose fibres with cellulose I crystal structure suggests the potential to make crystalline fibres directly from kraft pulp. The peak shifts observed in Figure 38 could be due to a change in the lattice spacing (d) between the planes during the dissolution and electrospinning processes. According to Bragg's Law[110]:

$$d = \frac{\lambda}{2 \cdot \sin \theta} \qquad \text{(Equation 4.2.4.1)}$$

Where: λ = wavelength of X-rays (in this case, CuKα, λ=0.154nm)

d = lattice spacing between the planes

θ = angle between the incident ray and the scattering planes.

Table 13 shows that the calculated lattice spaces between the planes in electrospun fibers are larger than the lattice spacing between the planes in kraft pulp.
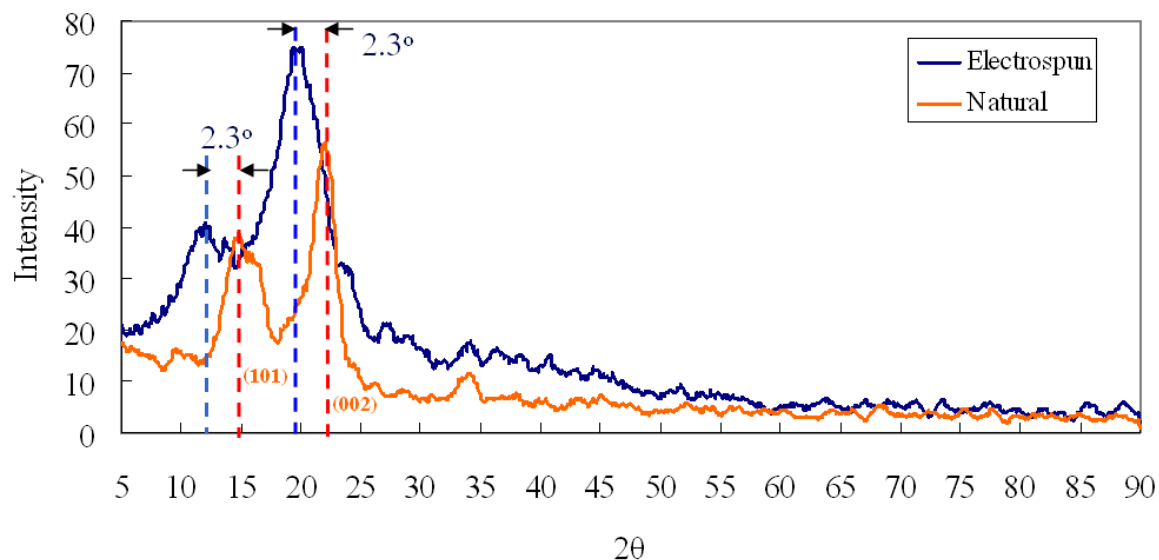
Figure 38. XRD of kraft pulp and electrospun fibres

Table 13. 2θ values, corresponding planes and lattice spacing between the planes of kraft pulp and electrospun fibers

	2θ (°)		Lattice spacing (nm)	
Sample	(101)	(002)	$d_{(101)}$	$d_{(002)}$
Kraft Pulp	14.9	22.0	0.594	0.404
Electrospun Fibers	12.6	19.7	0.702	0.450

4.3 Chemical Characterization

4.3.1   Carbohydrate Analysis

Both the raw pulp and electrospun fibres were subject to a carbohydrate analysis to determine their sugar content (glucose, xylose and mannose). Glucose is the major component of cellulose. Xylose and mannose are the components of hemicellulose. The carbohydrate analysis results are summarized in Table 14. The hemicellulose (xylose and mannose) content in the electrospun fibres averaged 5.1%, which is less than the 12.1% average in raw pulp. However, the difference in the hemicellulose content between kraft pulp and electrospun fibres is not considered significant because hemicellulose is amorphous and does not affect the physical properties of the cellulose fibres as significantly as does the cellulose content. The cellulose content, which accounts for the crystalline region of the fibres, is nearly identical between kraft pulp and electrospun fibres at 86-87%. The difference of 5wt% in the recovery (wt%) between kraft pulp and electrospun fibres could be due to the presence of impurities (e.g. chromophores) in the solutions that produced during the electrospinning process.

Table 14. Results from carbohydrate analysis of kraft pulp and electrospun fibres

	Cellulose (wt%)	Hemicellulose (wt%)	Recovery (wt%)
Kraft Pulp	85.5±2.3	12.1±0.3	97.5±2.6
Electrospun Fibers	87.1±2.1	5.1±0.9	92.2±4.2

4.3.2   Energy-dispersive X-ray (EDX) Spectroscopy

SEM images of the fibre cross-section in Figure 31 show that the electrospun fibres have a skin-core microstructure. EDX spot analysis was done on the fibre skin and core to investigate whether there is a difference in the elemental composition, as shown in Figure 39.
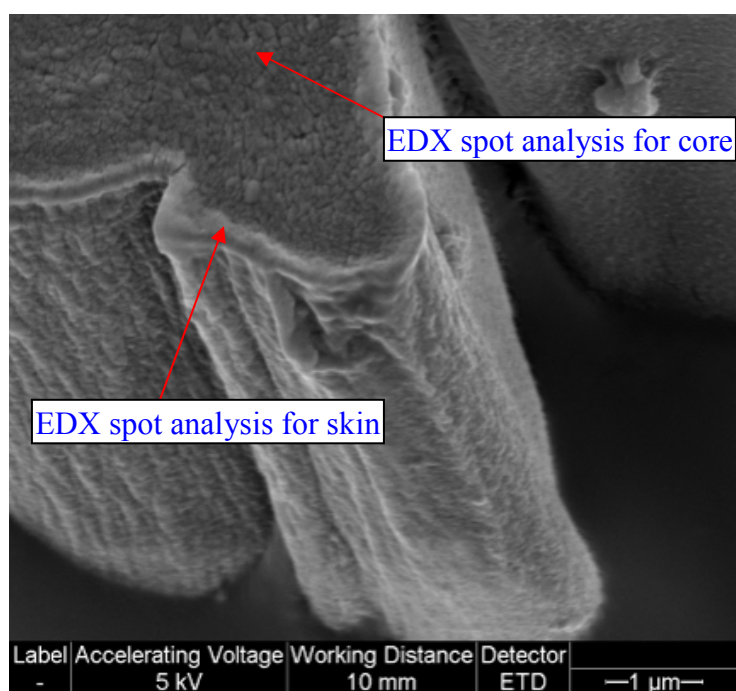
Figure 39. SEM image showing fibre skin and core locations for EDX analysis

EDX analysis was carried out and repeated three times on the different regions where the apparent fibre skin and core were located. Results from EDX analysis in Figure 40 and Figure 41 show that there are 80wt% of carbon and 20wt% of oxygen in the fibre skin and 78wt% of carbon and 22wt% of oxygen in the fibre core, indicating that there appears to be no difference in the elemental composition between the fibre skin and core. This

implies that the skin and core could have the same chemical composition but different material properties such as density. However, it was not known whether the x-rays could have penetrated through the fibre skin, thereby producing chemical composition data that would not be reflective of the actual fibre skin. Further characterization, including Auger electron spectroscopy, will have to be carried out to obtain a more detailed and accurate analysis of the chemical composition.
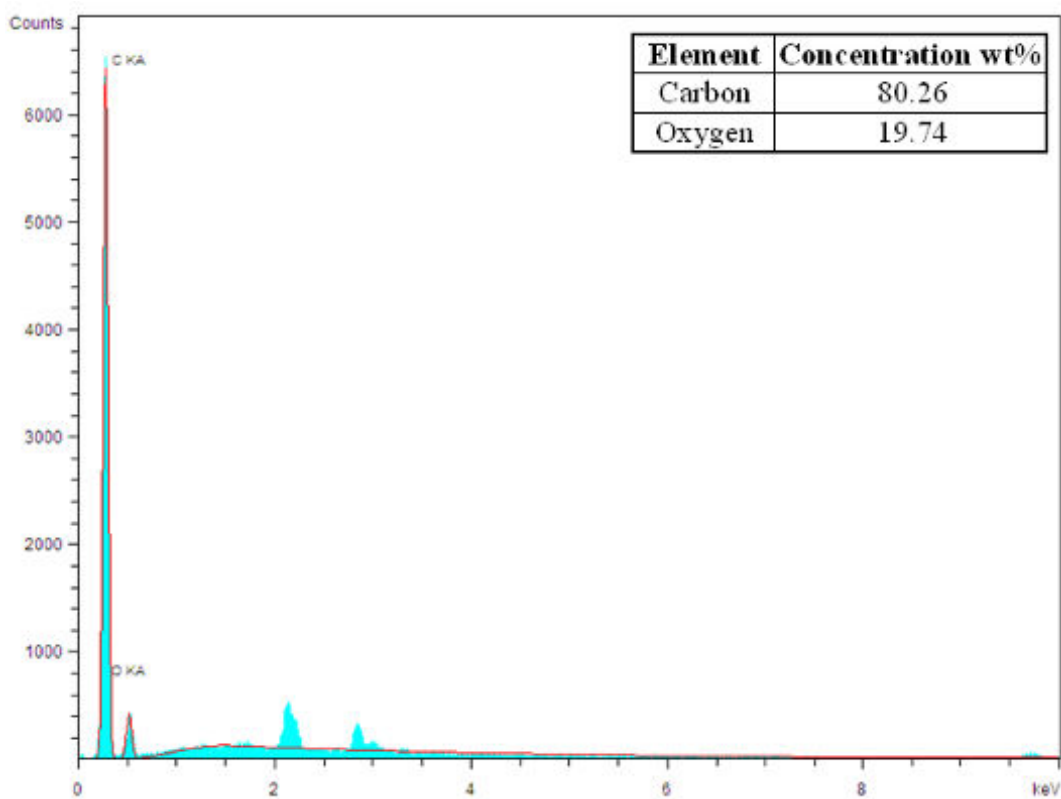
Figure 40. EDX spot analysis of the electrospun fibre skin

Element	Concentration wt%
Carbon	78.24
Oxygen	21.76
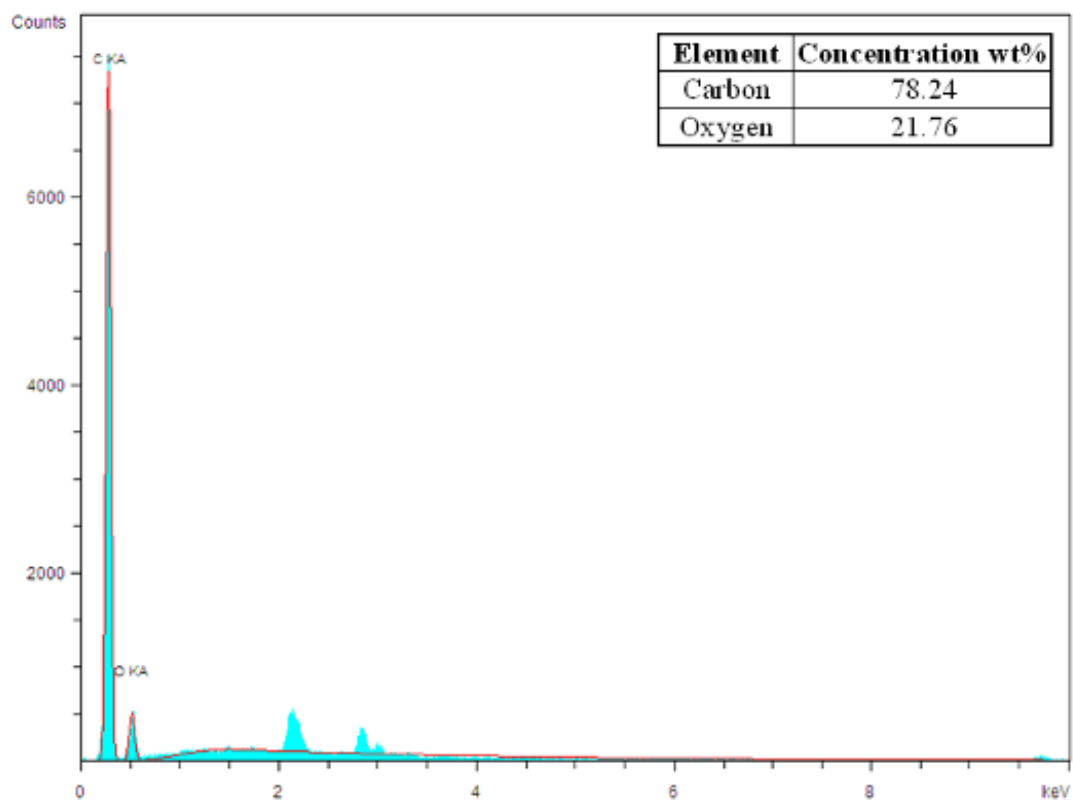
Figure 41. EDX spot analysis of the electrospun fibre core

4.4   Physical Characterization

4.4.1   Thermogravimetric Analysis (TGA)

The thermal behavior of the fibres could be affected by the degree of crystalinity as well as the molecular chain orientation of the fibres. An increase in either the degree of crystalinity or the molecular chain orientation is associated with increases in the thermal stability.[111] TGA was used to determine whether there is a difference in the thermal behavior between kraft pulp and electrospun fibres. From Figure 42, there is no significant difference in the thermal behavior between kraft pulp and electrospun fibres. The TGA results of commercial regenerated cellulose fibres including Lyocell, modal and viscose as reported by Carrillo et al. are shown in Figure 43.[112] The thermal degradation patterns of kraft pulp, electrospun fibres, and the commercial cellulose fibres are too similar to each one another .to identify any significant trends.
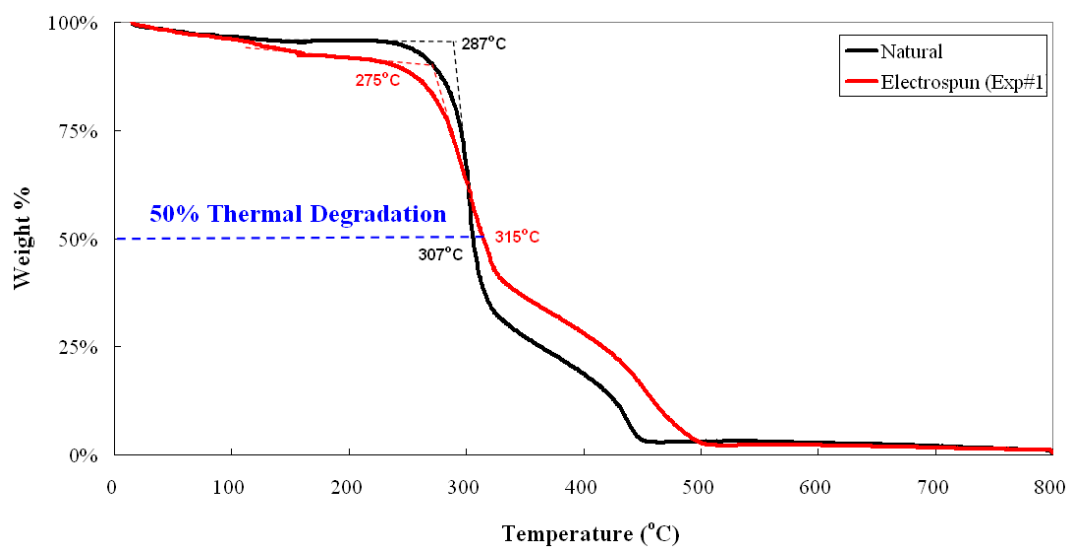
Figure 42. TGA results of kraft pulp and electrospun fibres

Table 15. Degradation temperatures of kraft pulp and electrospun fibres

Sample	Degradation Onset Temperature (^{o}C)	50% Thermal Degradation Temperature (^{o}C)
Kraft Pulp	287	307
Electrospun Fibres	275	315
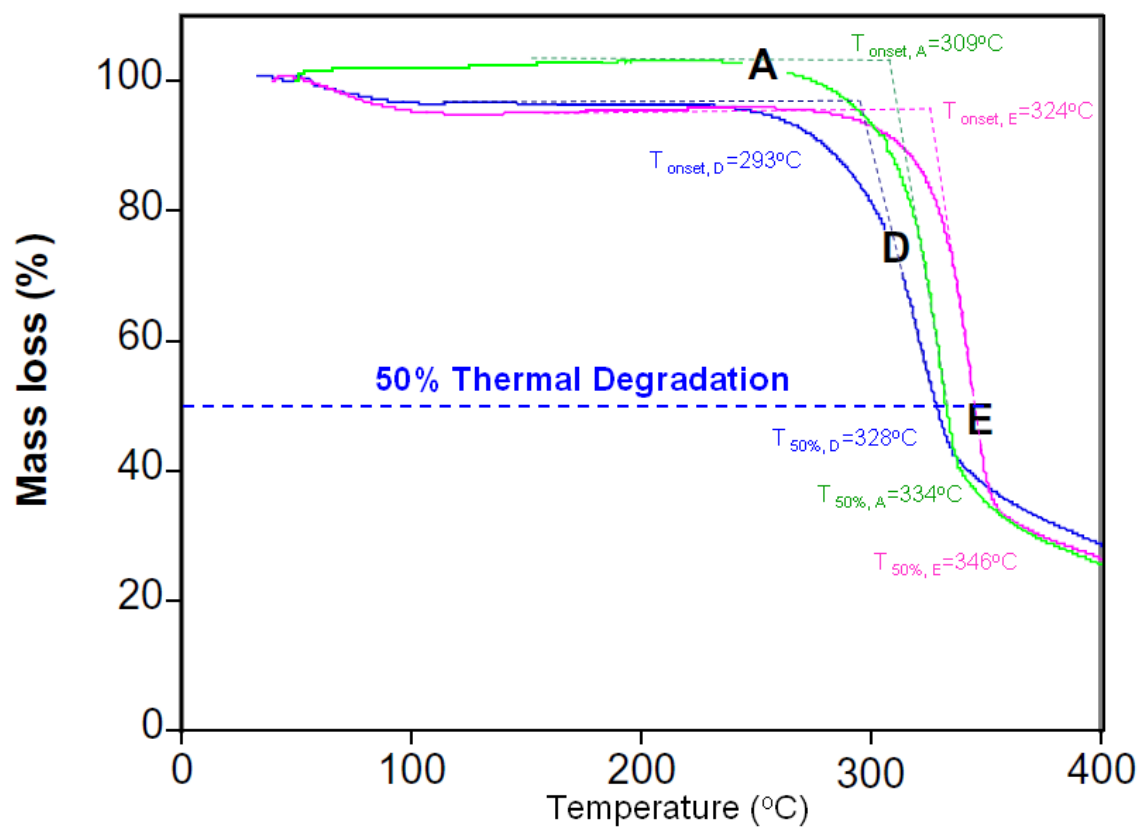
Figure 43. TGA patterns of the Lyocell (A), modal (D) and viscose (E) [112]

4.4.2   Differential Scanning Calorimetry (DSC)
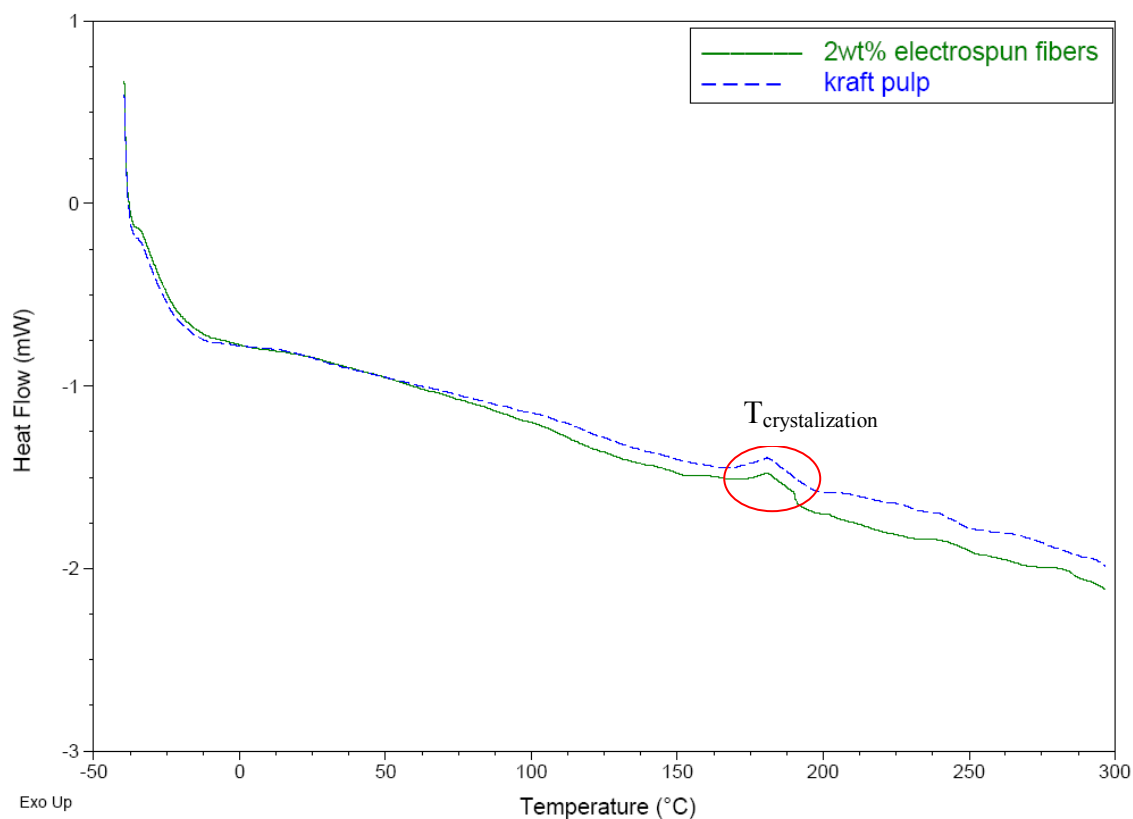
Figure 44. DSC results of kraft pulp and electrospun fibres

Both the electrospun fibres and kraft pulp were analyzed by DSC to examine whether there was any change in the phase transitions, including melting, crystallization and exothermic decomposition, as a result of the electrospinning process. The heat flow profiles of kraft pulp and electrospun fibres appear very similar to each other in Figure 44, with the crystallization temperature of both samples appearing at approximately 280°C, indicating that there is no significant change in the phase transition temperatures due to the cellulose dissolution process and the electrospinning process.

4.4.3   Contact Angle Measurements

Contact angle (θ_c) is the angle at which a liquid/vapor interface intersects with the solid surface (Figure 45). For a given system, the contact angle is determined by the interactions across the three interfaces. To measure the contact angle, a small liquid droplet is dropped on a flat horizontal solid surface as shown in Figure 45. The contact angle is a measure of the hydrophobicity (or wettability) of a surface. The more hydrophobic a surface is, the larger the contact angle. On surfaces that are highly hydrophobic, the water contact angles can be as high as 150° or even nearly 180°.[113] Wettability is crucial for fibre manufacturing, processing and applications. The highly polar nature of cellulose (thus hydrophilic) makes it poorly compatible with common non-polar polymers used in the production of textiles and composites. The ability to produce hydrophobic regenerated cellulose fibres, and thus those with improved compatibility with non-polar polymers, is expected to enhance the applications of cellulose fibres in the textile and composite industries. The mechanical properties of the hydrophobic regenerated fibres should be better than those of kraft pulp when exposed to the same moisture level due to a smaller extent of moisture absorption.
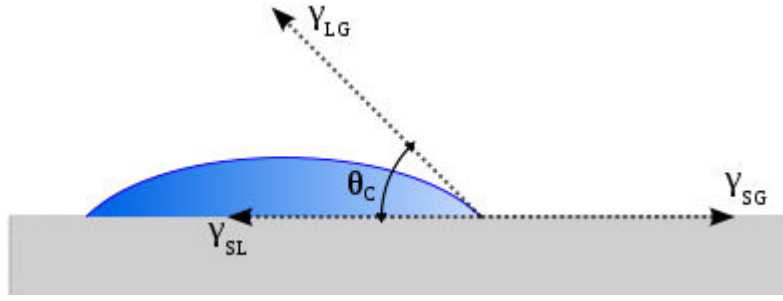
Figure 45. A contact angle of a liquid sample

To compute the non-equilibrium surface energy of the electrospun fibres (γ_{SG}), the following equations are used[114],[115]:

Young's Equation: $\gamma_{SG} = \gamma_{SL} + \gamma_{LG}\cos\theta_c$ (Equation 4.4.3.2)

Equation of State: $\gamma_{SL} = \gamma_{SG} + \gamma_{LG} - 2(\gamma_{SG}\gamma_{LG})^{1/2} \cdot e^{-\beta(\gamma_{SG}\gamma_{LG})^2}$ (Equation 4.4.3.3)

Where: γ_{SG} = interfacial tension between solid and gas

γ_{SL} = interfacial tension between solid and liquid

γ_{LG} = interfacial tension between liquid (water) and gas (air) = 72.8 dynes/cm

θ_c = contact angle

β = 0.0001247

The non-equilibrium surface energy of the electrospun fibres is computed by simultaneously solving Equation 4.4.3.2 and Equation 4.4.3.3.

Table 16 summarizes the contact angle measurements and the corresponding non-equilibrium surface energies of the electrospun fibres. As contact angle decreases

over time, the non-equilibrium surface energy increases, indicating an increase in the
interfacial tension between electrospun fibres and water with time.

Table 16. Contact angle and non-equilibrium surface energy of electrospun fibres

	t=0s	t=5s	t=30s	t=60s	t=300s
Contact Angle θ	105	100	82	75	61
Surface Energy (dynes/cm)	20.03	23.04	34.23	38.61	47.23

t=-1s   t=0s   t=1s
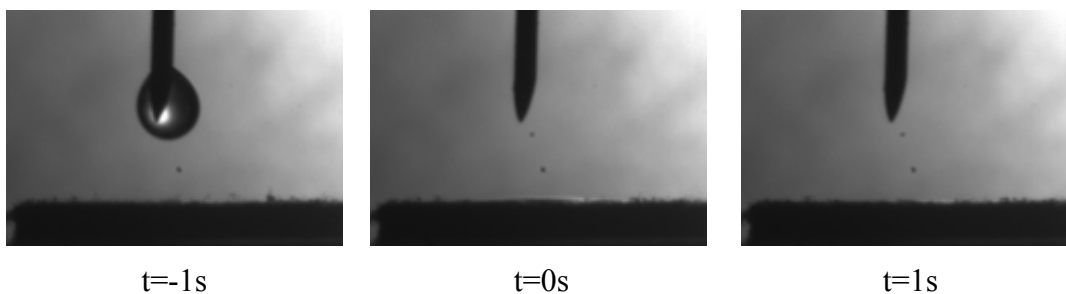
Figure 46. Snapshots of complete wetting of a water droplet on a mat covered with kraft pulp in powder form (0.5mm) at -1s, 0s, and 1s

t=0s, $\theta_c = 105^o$ t=5s, $\theta_c = 100^o$ t=30s, $\theta_c = 82^o$

t=1min, $\theta_c = 75^o$ t=5min, $\theta_c = 61^o$
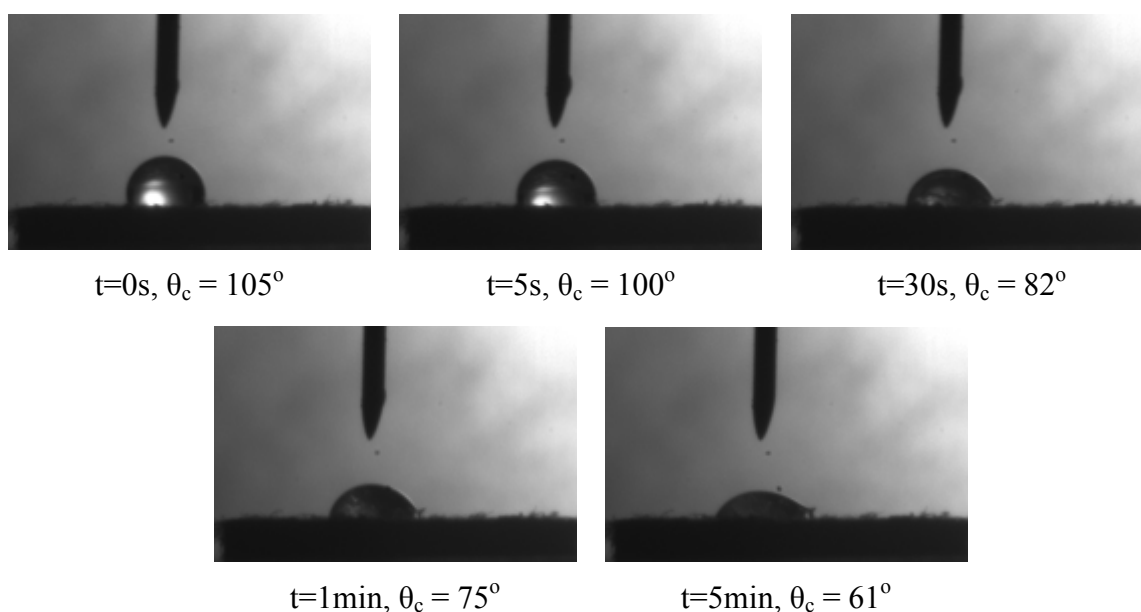
Figure 47. Snapshots of a water droplet on a mat covered with electrospun fibres in powder form (0.5mm) at 0s, 5s, 30s, 1min and 5min

Figure 46 and Figure 47 show how the water contact angle changes over time on the mats covered with kraft pulp and electrospun fibres in powder form. The results from the contact angle measurements indicate that the electrospun fibres are more hydrophobic than the natural kraft pulp. For the electrospun fibres, the water droplet can still be seen on the fibre surface after 5 minutes (Figure 47). For the natural kraft pulp, the water is completely absorbed by the fibres after 1 second, showing complete wetting on the kraft pulp fibre surface (Figure 46).
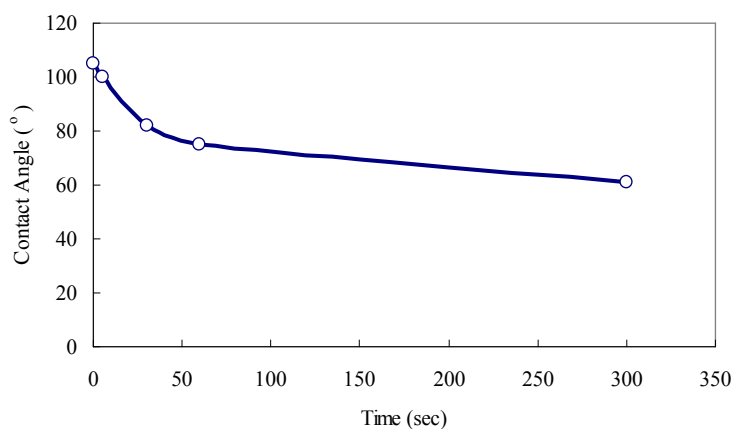
Figure 48. Contact angle of electrospun fibres versus time
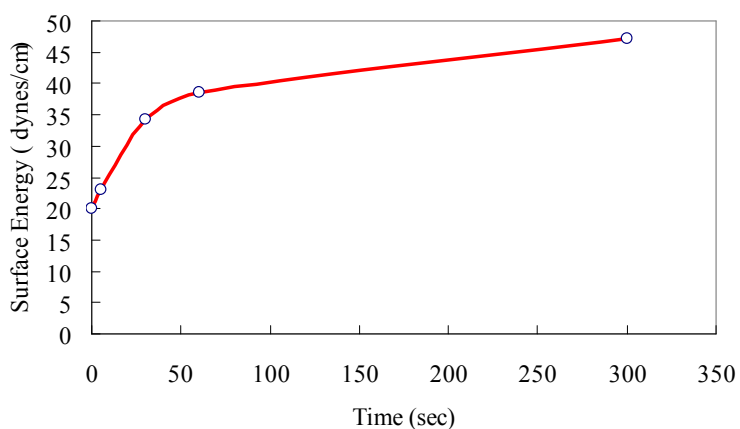
Figure 49. Non-equilibrium surface energy of electrospun fibres (Sample 1) versus time

The ability of the cellulose fibres to adsorb low molecular weight compounds (e.g. water) is a function of the primary chemical structure and the resulting microstructure, including the size of crystalline and amorphous regions, porosity, the microfibrilar structure as well as the surface morphology.[116]   The difference in the hydrophobicity of kraft pulp and electrospun fibres could be due to changes in both the primary chemical structure and the microstructure.

Effect of Primary Chemical Structure on Hydrophobicity

IR spectra in Section 4.2.3 indicate that the hydrophilic hydroxyl (-OH) groups have become less accessible compared to those in kraft pulp. This could be a contributing factor causing the electrospun fibres to be more hydrophobic than kraft pulp.

Effect of Microstructure on Hydrophobicity

SEM images of kraft pulp and electrospun fibres in powder form (0.5mm) are shown in Figure 50. There is no significant difference, as expected, in the general fibre morphology between kraft pulp and electrospun fibers, given that both samples were prepared using the same procedure. One possible explanation involves the water accessibility to the hydrophilic groups (e.g. hydroxyl groups). Electrospun fibres have a fibrillation-free fibre surface (Figure 51) and kraft pulp fibres have a fibrillated fibre surface (Figure 52). Having a fibrillated surface morphology leads to an increase in the fibre specific surface area, which subsequently contributes to the hydrophilicity of kraft pulp. SEM images in

Figure 53 show that the electrospun fibres have a solid structure, as opposed to the kraft pulp fibres which have a hollow tubular structure like other wood fibres, as shown in Figure 54[117]. The solid structure of electrospun fibres should make water less accessible to the hydroxyl groups compared to kraft pulp, which has a hollow structure. Surface porosity, which is related to the specific surface area, could be another contributing factor to the hydrophobic nature of the fibres. Electrospun fibres appear to have a better-packed fibre skin than kraft pulp. This suggests that electrospun fibres may have fewer voids and thus lower porosity. However, the difference in porosity between the two samples will have to be confirmed with further studies using porosimetry techniques. Figure 55 illustrates the apparent microstructures of electrospun fibre and kraft pulp fibre based on observations from the SEM images in Figure 51 and Figure 52 and the literature image in Figure 54.
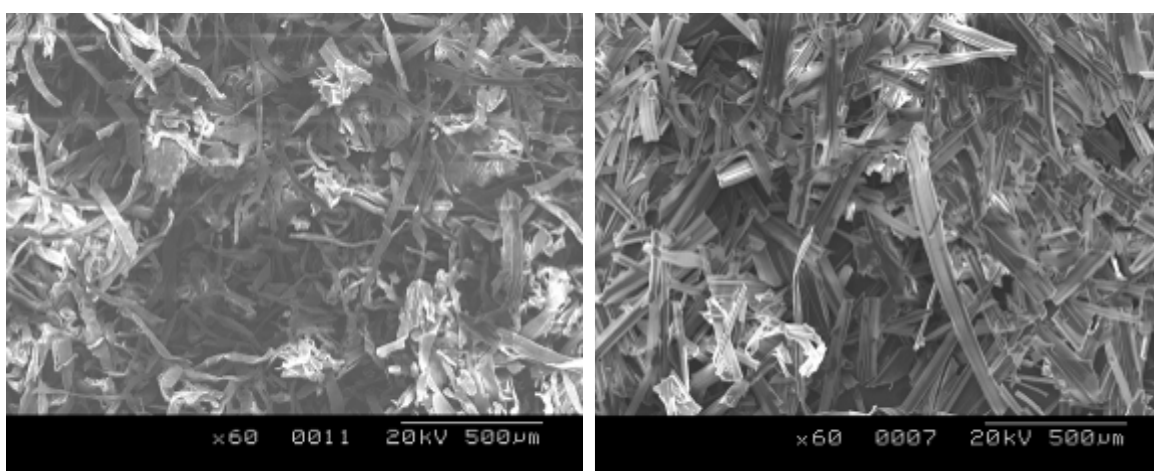
Figure 50. SEM images of kraft pulp (left) and electrospun fibres (right) in powder form (0.5mm). Scale bar: 500um
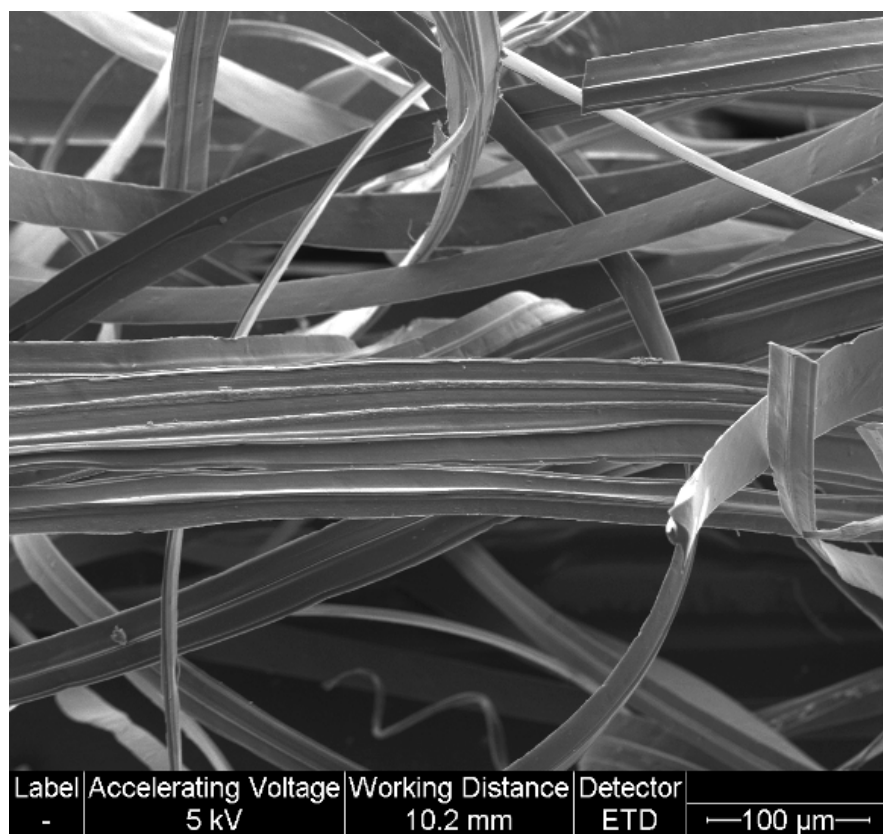
Figure 51. SEM of electrospun fibres showing the fibrillation-free surface morphology

Figure 52. SEM of kraft pulp showing the fibrillated surface morphology
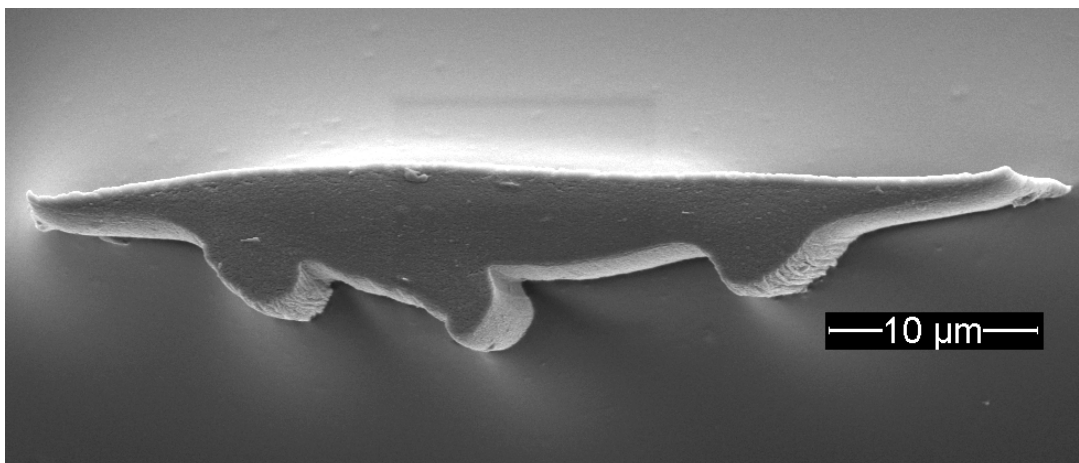
Figure 53. SEM image showing the solid core of an electrospun cellulose fibre
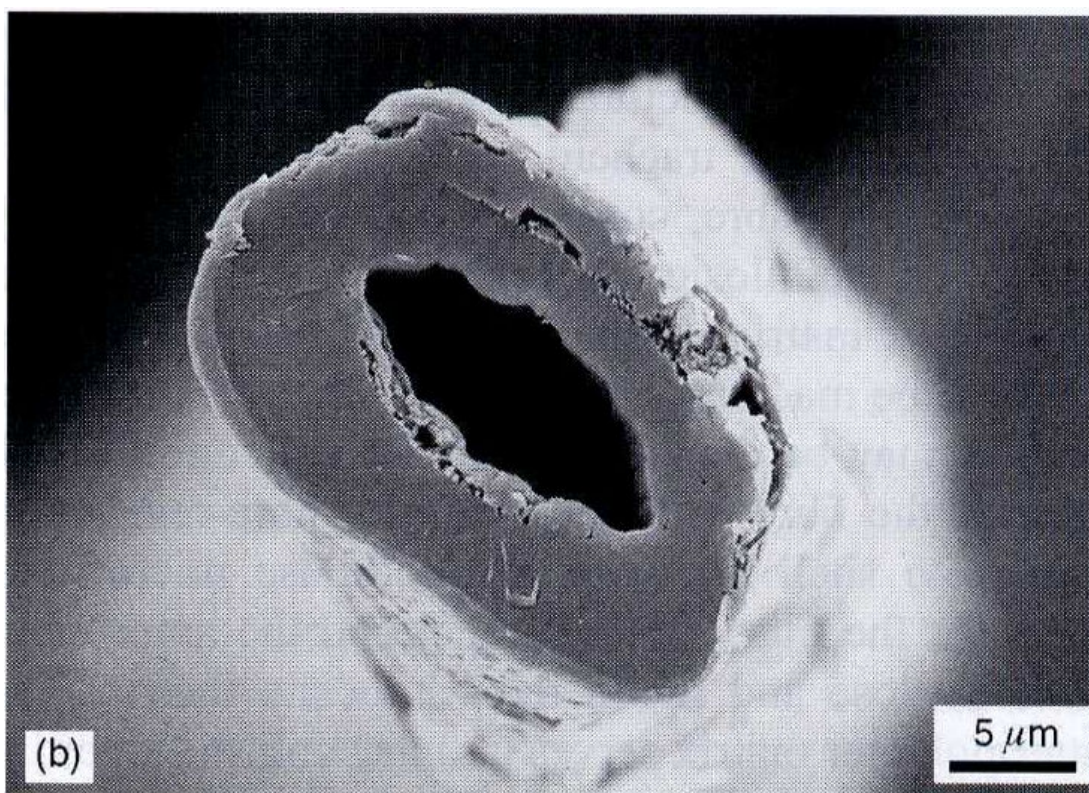
Figure 54. SEM image depicting the hollow tubular cross-section of a softwood fibre (*Pinus banksiana*) [117]
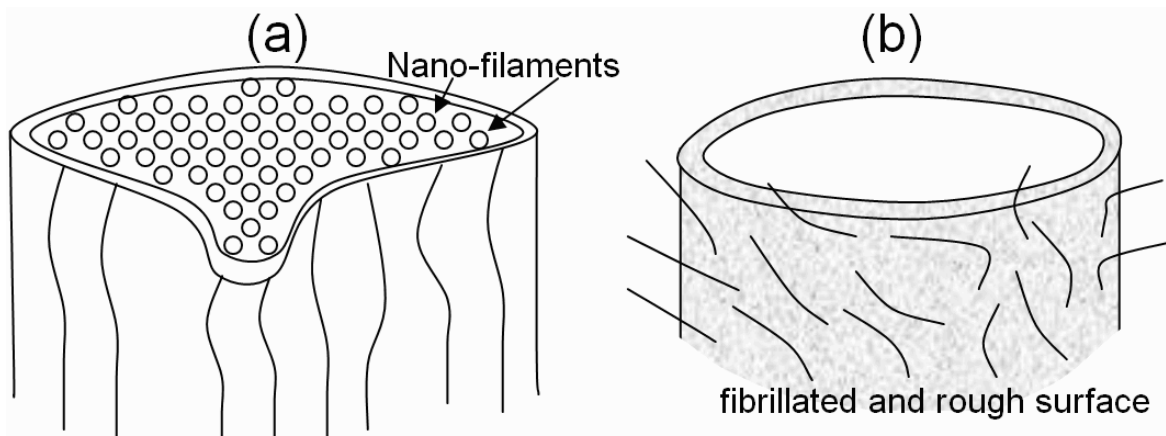
Figure 55. Illustrations showing the microstructures of (a) the electrospun fiber (solid core and non-fibrillated, smooth skin) and (b) kraft pulp fibre (hollow core and fibrillated, rough skin)

4.5   Mechanical Characterization

4.5.1   Microtensile Testing

Tensile testing was conducted on 50 samples of the electrospun fibres from Experiment 1 to characterize the mechanical properties. The load-displacement curves of 10 of the 50 samples are shown in Figure 56. There appears to be a significant variation in the mechanical behavior of the electrospun single fibres. The mechanical testing results are consistent with the SEM (Figure 31) and confocal microscopy (Figure 35) observations in that there is a large variation in the fibre geometry for individual fibres. This indicates that the electrospinning process needs to be further optimized to improve the consistency of the electrospun fibre geometry before the mechanical properties of the electrospun fibres can be fully characterized.
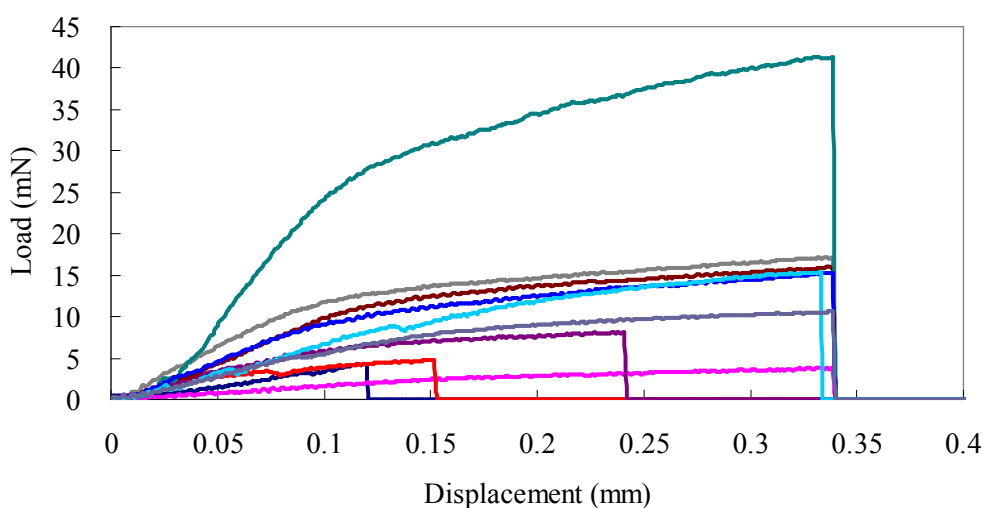
Figure 56. Load-displacement curves of electrospun single fibres

Based on the confocal micrographs, the average electrospun fibre cross-sectional surface area is $117 \pm 50 \mu m^2$. To conduct a preliminary study on the electrospun fibres' mechanical properties, stress-strain curves of the 10 samples (Figure 57) were obtained by normalizing the breaking load with the average electrospun fibre cross-sectional surface area of $117 \mu m^2$. Based on the stress-strain curves of the 50 samples, the preliminary mechanical properties of the electrospun fibres are summarized in Table 17.
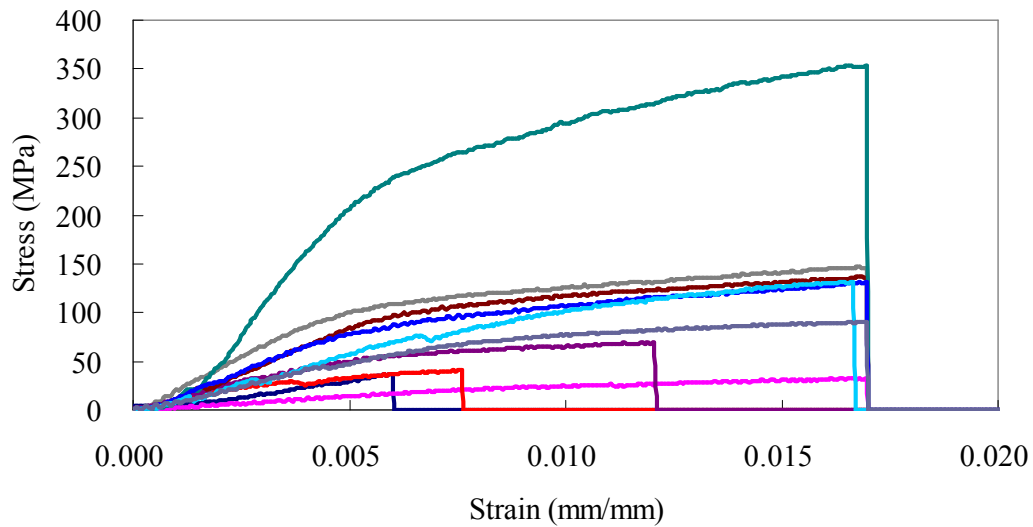
Figure 57. Stress-strain curves of electrospun single fibres

Table 17. Mechanical properties of the electrospun single fibres

Average Breaking Strength (MPa)	151 ± 121
Average Modulus (GPa)	14 ± 11
Average Strain (%)	1.7 ± 0.4

The breaking strength of the electrospun fibres (sample size = 50) has an average value of 151MPa with a standard deviation of 121MPa, showing a significant variability, which is due to the large variation in the actual fibre cross-sectional area. The two-tailed Student's t-test method was used to determine the confidence intervals of the population mean strength (μ) at various confidence levels.

$$t = \frac{\bar{x} - \mu}{S_n / \sqrt{n}} \qquad \text{(Equation 4.5.1.1)}$$

Confidence interval: $\bar{x} - t_{\alpha/2} \dfrac{S_n}{\sqrt{n}} < \mu < \bar{x} + t_{\alpha/2} \dfrac{S_n}{\sqrt{n}}$ (Equation 4.5.1.2)

Where:

$\bar{x}$ = sample mean

μ = population mean

$t_{\alpha/2}$ = two-tailed student's t-test value

n = sample size

S_n = standard deviation

α = 1 - confidence level

From Equation 4.5.1.2, the confidence intervals of the population mean strength at various confidence levels were calculated and summarized in Table 18. For a 90% confidence level, the confidence interval of the population mean strength is 122MPa < μ < 180MPa.

Table 18. Confidence intervals of the population mean strength at different confidence levls based on the two-tailed Student's t-test method

Confidence level	t	μ_{min} (MPa)	μ_{max} (MPa)
75%	1.164151	131	171
90%	1.676551	122	180
95%	2.009575	117	185
99%	2.679952	105	197

5   CONCLUSION

In this study, it has been successfully demonstrated that regenerated cellulose fibres can be produced using a one-step electrospinning process directly from kraft pulp. Solvent spinning (e.g. viscose process) would normally require processing of the pulp into dissolving pulp. The ability to directly electrospin cellulose fibres from kraft pulp is significant because the processing cost can be reduced and there is great potential of finding a new route to product development for kraft pulp manufacturers. The NMMO process was used in this study because of its commercial feasibility and the potential to develop a closed-loop, environmentally friendly fibre-making process. Based on the design of experiments and Response Surface Analyses, the optimum conditions for producing single fibres from the electrospinning process are 2wt% cellulose concentration, $100^{o}C$ ambient temperature, and 5kV of voltage, as indicated by Experiment 1. Only electrospun fibres from Experiment 1 could be hand-pulled for single fibre collection, while the remaining 17 experiments produced either no fibres or fine fibres that were prone to breaking upon hand-pulling, suggesting the need to improve the fibre take-up mechanism of the electrospinning process.

The results from intrinsic viscosity measurements indicated that the degree of cellulose polymerization in the electrospun fibres is close to 600, compared to 1000 in kraft pulp. The electrospun fibre DP is in good agreement with the commercial cellulose fibre

(Lyocell), which also has a DP of 600, indicating that this is a sufficiently long molecular chain structure for electrospinning.

SEM observations indicated that micron- and submicron-scale cellulose fibres could be produced from kraft pulp using the electrospinning process. However, a suitable fibre take-up is needed to collect the submicron-fibres in a single fibre form or as a fibrous mat. Observations from SEM and confocal microscopy revealed that the electrospun fibres from kraft pulp have varying cross-sectional shape and surface area, suggesting that further optimization is necessary for the electrospinning process. Similar to other solvent-spun cellulose fibres, including viscose and Lyocell, an apparent skin-core microstructure of the electrospun fibres is observed under SEM. This observation is important because the skin-core microstructure has been shown to be detrimental to the mechanical properties of the other regenerated cellulose fibres. Unlike viscose and Lyocell, external fibrillation is not observed in the electrospun fibres. SEM images also show that the electrospun fibres appear to have a nano-filament structure in the fibre core. The absence of external fibrillation and presence of a nano-filament structure suggest that the electrospinning process could potentially produce high-quality regenerated cellulose fibres.

A comparison between the infra-red spectra of both kraft pulp and electrospun fibres indicates that the cellulose in the electrospun fibres was not derivatized during the

dissolution and electrospinning processes and that the original cellulose chemical structure is largely preserved in the electrospun fibres. However, the band corresponding to the hydroxyl (-OH) groups' bending mode appears to have become less prominent compared to kraft pulp. This suggests (1) there could be bridging of the inter-molecular chain hydroxyl groups or (2) the concentration of hydroxyl groups in electrospun fibres could have been reduced. Based on the X-ray Diffraction analysis, the electrospun fibres appear to have a Cellulose I crystal structure. This is an indication that crystalline cellulose I fibres can be produced by the electrospinning process. Carbohydrate analysis showed that the chemical composition (in terms of sugar contents) of kraft pulp and electrospun fibres does not appear to be significantly different. The results from Energy Dispersive X-ray analysis indicate that there appears to be no significant difference in the elemental compositions of the fibre skin and core. Further analyses will need to be carried out to obtain a more detailed understanding of the structure and composition of the electrospun fibres.

Thermogravimetric analysis suggested that there appears to be no significant difference in the thermal behavior between kraft pulp and electrospun fibres. The results of differential scanning calorimetry showed that there is no significant difference in the phase transition temperatures between kraft pulp and electrospun fibres, indicating that the polymeric bacbone structure remained virtually unchanged after the dissolution and electrospinning processes. However, contact angle measurements indicated that electrospun fibres (contact

angle = 105° at t=0s) appear more hydrophobic than kraft pulp (contact angle =0° at t=0s), which could be due to the better-packed electrospun fibre surface and the apparently less predominant hydrophilic hydroxyl groups, as indicated by the IR study.

Microtensile testing was done on 50 samples from Expt. 1 fibres. The results showed that there was a large variability in the fibres' mechanical properties, which is consistent with the large variations in the electrospun fibre cross-sectional shape and surface area. With an improved electrospinning setup, process control and post-treatment, better consistency in the fibre cross-sectional surface area would be expected, resulting in high-quality cellulose fibres with less fluctuating mechanical properties potentially being derived from kraft pulp using the electrospinning process. This is significant because the pulp manufacturers will benefit from the ability to produce cellulose fibres with controlled moisture resistance and improved mechanical properties directly from kraft pulp. By using electrospun cellulose fibres from kraft pulp, there is potential to develop high value-added products, including high-performance textile materials (e.g. bullet-proof vests) and reinforcement fibres for composite applications.

6   FUTURE WORK

The varying electrospun fibre cross-sectional shape and surface area indicated by SEM and confocal microscopy are a clear indication that optimization of the electrospinning process conditions is needed to gain better control over key product parameters. Temperature control, fibre coagulation, and fibre collection are three areas of potential improvement that will enhance the reproducibility and consistency of the electrospinning process. The current electrospinning setup uses a heat gun to heat up the temperature from 20 to $100\text{-}140^{\text{o}}\text{C}$ in an open environment. Air turbulence from the heat gun and temperature changes in the open environment introduces unnecessary variables into the electrospinning process. Ideally, ambient temperature should be accurately controlled with a static heat source (for example laser gun and oven) in a sealed environment so that the electrospun fibre diameter and other properties (for example tensile strength) could be better controlled. Fibre coagulation is important for the formation of the fibre morphology and the properties. The coagulant type, coagulant temperature, salt content, number of washes and several other variables would be expected to affect the fibre coagulation process. Fibre collection of the current electrospinning setup is another area that requires improvement. It has been demonstrated that submicron-scale electrospun fibres can be produced but cannot be collected in a separable form. Having an effective fibre collection mechanism would allow the submicron-scale electrospun fibres to be collected as a random fibre mat. Drawing, which is a critical step in determining the fibre structure and

116

properties, was not included in the current setup. Experiments were carried out to introduce a draw ratio to the wet electrospun fibres using two fibre take-up units operating at different rotational speeds. However, the wet electrospun fibres were prone to breaking during the drawing process. A well-designed fibre drawing and winding mechanism is thus needed to collect electrospun fibres with better-controlled dimensions and thus more consistent fibre properties.

To better establish the structure-property-process relationships of the electrospun fibres, several characterization techniques discussed in the previous sections should be repeated and expanded. Other characterization techniques that were not described in this work should also be used. Transmission electron microscopy can be used to study the fibre surface and cross-sectional morphology on the nano-scale. Infra-red spectroscopy should be repeated for the kraft pulp and electrospun fibres to include the 2000-4000cm^{-1} wavelength range so that a complete analysis of their chemical structure can be conducted. Raman spectroscopy can be applied to carry out a complementary vibrational spectroscopy study of the electrospun fibres' chemical structure. Auger electron spectroscopy perhaps could reveal differences between the electrospun fibres' skin and core elemental compositions. To relate the wettability to structural properties, mercury porosity and the Brunauer-Emmett-Teller (BET) method should be performed on kraft pulp and electrospun fibres, which would measure the porosity of the fibres and determine the specific surface area of the fibres, respectively. After electrospun fibres with

better-controlled fibre geometry were produced, microtensile testing could be conducted to characterize the mechanical properties of the electrospun fibres.

Fibre post-treatments, including drawing and heat treatment, could be carried out to improve the mechanical properties of the fibres. Drawing of the fibres can improve the molecular chain alignment, leading to more crystalline regions in the fibres and a higher tensile strength. Heat treatments allow recrystallization to occur within the fibres, thereby increasing overall crystalinity of the fibre.

If electrospun fibres could be produced under well-controlled electrospinning conditions, they then could be carbonized into carbon fibres. The non-petroleum-based electrospun carbon fibres from kraft pulp could potentially be developed to replace the current generation of oil-derived carbon fibres. This has potential of leading to the development of a wide range of applications for the electrospun fibres from kraft pulp.

REFERENCES

[1] Cuculo, J., Aminuddin, N., Frey, M. W., "8. Solvent Spun Cellulose Fibres" in Structure Formation in Polymeric Fibres. Hanser Gardner Publications: Munich, 2001

[2] Alkaline Pulping, Pulp and Paper Manufacture, Vol. 5, 3rd Ed., Technical Session of Canadian Pulp and Paper Association, 1989

[3] Biermann, C. J., Essentials of Pulping and Papermaking. San Diego: Academic Press, Inc., 1993

[4] Statistic Canada. Accessed on October 27, 2008 from
<http://cansim2.statcan.gc.ca/cgi-win/cnsmcgi.pgm>

[5] Zhang, Y., Lim, C. T., Ramakrishna S., Huang, Z-M., Journal of Materials Science: Materials In Medicine, 16, 933– 946, 2005

[6] Curtis, A., C. Wilkinson, C., Trends Biotechn., 19, 3, 97, 2001

[7] Hamad, W., The Canadian Journal of Chemical Engineering, Vol 84, 2006

[8] Polymer Handbook 4th Edition, 1999.

[9] Hiltunen, E., PhD Thesis, Helsinki University of Technology, 2003

[10] Hamad, W., The Canadian Journal of Chemical Engineering, Vol 84, 2006

[11] Reneker, D. H., Chun, I., Nanotechnology, 7, 216, 1996.

[12] Frey, M.W., Polymer Reviews, 48:378–391, 2008

[13] Doshi, J., Reneker, D. H., J Electrostatics, 35(2-3):151–60, 1995

[14] Wilkes, A., Chapter 3. The Viscose Process, Regenerated Cellulose Fibres, Woodhead Publishing, 2001

[15] Frey, M.W., Polymer Reviews, 48:378–391, 2008

[16] Neagu, R.C., Gamstedt, E.K., Bardage, S.L., Lindstrom, M., Wood Material Science and Engineering, 1, 146-170, 2006

[17] Nevell, T. P., Zeronian, S. H., Cellulose Chmistry and Its Applications, 1985

[18] Tripp, V., Conrad, C., Chapter 5 X-ray Diffraction, Instrumental Analysis of Cotton Cellulose and Modified Cotton Cellulose, Edited by R. O'Corner, Marcel Dekker Inc., New York, 1972.

[19] Woodings, C., Regenerated Cellulose Fibres, Chapter 1, p.14, 2001

[20] Kotek, R., Handbook of Fibre Chemistry 3rd Edition, Regenerated Cellulose Fibres, Chapter 10, 667-771, 2007

[21] Kotek, R., Handbook of Fibre Chemistry 3rd Edition, Regenerated Cellulose Fibres, Chapter 10, 667-771, 2007

[22] Rosenau, T., Elder, T., Potthast, A., Sixta, H., Kosma, P., 12th International Symposium on Wood and Pulping Chemistry, p.305-308, 2002

[23] Case, F., Inform, 16:179, 2005

[24] Kulpinski, P., Journal of Applied Polymer Science, Vol. 98, 1855–1859, 2005

[25] Dupont, A.-L., Polymer, 44, 4117-4126, 2003

[26] Dawsey, T.R., McCormick, C.L., J. Macromol. Sci. – Rev. Macromol. Chem. Phys., C30: 405 -440, 1990

[27] Kim, C.W., Kim, D.S., Kang, S.Y., Marquez, M., Joo, Y.L., Polymer, 47, 5097-5107, 2006

[28] Kotek, R., Handbook of Fibre Chemistry 3rd Edition, Regenerated Cellulose Fibres, Chapter 10, 667-771, 2002

[29] Nevell, T. P., Zeronian, S. H., Cellulose Chmistry and Its Applications, 1985

[30] Dawsey, T.R., McCormick, C.L., J. Macromol. Sci. – Rev. Macromol. Chem. Phys., C30: 405 -440, 1990

[31] Dupont, A.-L., Polymer, 44, 4117-4126, 2003

[32] Sheldon, R. Chem. Commun., 23, 2399-2407, 2001

[33] Welton, T. Chem. ReV., 99, 2071-2083, 1999

[34] Murugesan, S.; Linhardt, R. J. Curr. Org. Synth., 2, 437-451, 2005

[35] Park, S., Kazlauskas, R. J. Curr. Opin. Biotechnol., 14, 432-437, 2003

[36] Swatloski, R.P., Spear, S.K., John, D., Holbrey, J.D., Rogers, R.D., J. Am. Chem. Soc., 2002, 124, 4974–4975.

[37] Kotek, R., Handbook of Fibre Chemistry 3rd Edition, Regenerated Cellulose Fibres, Chapter 10, 667-771, 2002

[38] Kotek, R., Handbook of Fibre Chemistry 3rd Edition, Regenerated Cellulose Fibres, Chapter 10, 667-771, 2002

[39] Zhu, S., Wu, Y., Chen, Q., Yu Z., Wang, C., Jin, S., Ding, Y., Wu, G., The Royal Society of Chemistry 2006, Green Chem., 8, 325-327, 2006

[40] Viswanathan, G., Murugesan, S. Pushparaj, V., Nalamasu, O., Ajayan, P.M., Linhardt, R.J., Biomacromolecules, Vol. 7, No. 2, 2006

[41] Nevell, T. P., Zeronian, S. H., Cellulose Chmistry and Its Applications, 1985

[42] Hudson, S.M., Cuculo, J.A., J. Polym. Chem. Ed., 20, 499, 1982

[43] Sangwatanaroj, U., M. Sc. Thesis, North Carolina State University, NC

[44] Hattori, K., Cuculo., J.A., Hudson, S.M., Journal of Polymer Science: Part A: Polymer Chemistry, Vol. 40, 601–611, 2002

[45] Hattori, K., Cuculo., J.A., Hudson, S.M., Journal of Polymer Science: Part A: Polymer Chemistry, Vol. 40, 601–611, 2002

[46] Frey, M. W.; Joo, Y.; Kim, C. "New solvents for cellulose electrospinning and preliminary electrospinning results", Abstracts of Papers of the American Chemical Society, 226, U404–U404, 2003

[47] Zimmermann, R.L., US Patent 5,216,154, 1993

[48] Franks, N.E., Varga, J.K., US Patent 4,145,532, 1979

[49] Wachsmann U, Diamantoglou M., Das Papier, 51(12):660-5, 1997

[50] Gagnaire, D., Mancier, D., Vincendon, M., J Polym Sci Polym Chem Ed 18, pp. 13–25, 1980

[51] Chanzy, H., Navrot, S., Peguy, A., Smith, P., Chevalier, J., J Polym Sci, Polym Phys Ed 20, pp. 1909–1924, 1982

[52] Berger, W., Keck, M., Philipp, B., Cell Chem Technol, 22, pp. 387–397, 1988

[53] Buijtenhuijs, F.A., Abbas, M., Witteveen, A.J.,. Das Papier 40 12, pp. 615–619, 1986

[54] Krässig, H.A., In: Huglin, M.B., Editor, Cellulose-structure, accessibility and reactivity, Gordon Breach, Yverdon, 1993

[55] Schweizer, E., J Prakt Chem, 72, 109, 1857

[56] Despeissis, L.H., France Patent, 203, 741, 1890

[57] Kotek, R., Handbook of Fibre Chemistry 3rd Edition, Regenerated Cellulose Fibres, Chapter 10, 667-771, 2002

[58] C C McCorsley and J K Varga, US patent 4 142 913, 1979

[59] Crooks, W., Electric Lamps & co, British Patent 2612, 1881

[60] Kamide, K., Nishiyama, K., Chapter 5. Cuprammonium Process, Regenerated Cellulose Fibres, Woodhead Publishing, 2001

[61] Despeissis, L.H., France Patent, 203, 741, 1890

[62] Wilkes, A., Chapter 3. The Viscose Process, Regenerated Cellulose Fibres, Woodhead Publishing, 2001

[63] C C McCorsley and J K Varga, US patent 4 142 913, 1979

[64] White, P. Chapter 4, Lyocell: The Production Process and Market Development, Regenerated Cellulose Fibres, Woodhead Publishing, 2001

[65] Huang, Z., Zhang, Y., Kotakic, M., Ramakrishna. S., Composites Science and Technology, 63, 2223-2253, 2003

[66] Doshi, J., Reneker, D. H., J Electrostatics, 35(2-3):151–60, 1995

[67] Formhals, A., Gastell, R. S., US Patent 1,975,504, 1934

[68] Cuculo, J. A., Aminuddin, N., Frey, M. W. Solvent spun cellulose fibres, In Structure Formation in Polymeric Fibres; Salem, D. R., Ed.; Hanser Publishers: Munich, pp. 296–328, 2000

[69] Kim, C.W., Kim, D.S., Kang, S.Y., Marquez, M., Joo, Y.L., Polymer, 47, 5097-5107, 2006

[70] Kim, C.W., Kim, D.S., Kang, S.Y., Marquez, M., Joo, Y.L., Polymer, 47, 5097-5107, 2006

[71] Kulpinski, P., Journal of Applied Polymer Science, Vol. 98, 1855–1859, 2005

[72] Kim, C.-W., Frey, M. W., Marquez, Manuel, Yong, L. J., Journal of Polymer Science: Part B: Polymer Physics, Vol. 43, 1673–1683, 2005

[73] Viswanathan, G., Murugesan, S. Pushparaj, V., Nalamasu, O., Ajayan, P.M., Linhardt, R.J., Biomacromolecules, Vol. 7, No. 2, 2006

[74] Frey, M. W.; Song, H. "Cellulose fibres formed by electrospinning from solution", Abstracts of Papers of the American Chemical Society, 225, U288–U288, 2003

[75] Ko, F., "Nanofibre Technology: Bridging the Gap between Nano and Macro World." NATO ASI on Nanoengineeered Nanofibrous Materials, 2003

[76] Yeoh, S.J., Louis, B., Ko, F., Poster Presentation, Cascadia Nanotech BC Conference 2008.

[77] Reneker, D. H., Chun, I., Nanotechnology, 7, 216, 1996

[78] Ayutsede, J., Gandhi, M., Sukigara, S., Ye, H., Hsu, C.-M., Gogotsi, Y., Ko, F., Biomacromolecules, 7, 208-214, 2006

[79] Zhang, Y., Lim, C. T., Ramakrishna S., Huang, Z-M., Journal of Materials Science: Materials In Medicine, 16, 933– 946, 2005

[80] Nakata, K., Fujii, K., Ohkoshi, Y., Gotoh, Y., Nagura, M., Numata, M., Kamiyama, M., Macromol. Rapid Commun., 28, 792–795, 2007

[81] Maschmanna, M.R., Amamab, P., Goyal, A., Iqbal, Z., Gat, R., Fisher, T.S., Carbon, Volume 44, Issue 1, Pages 10-18, 2006

[82] Ondarcuhu T, Joachim C., Europhys Lett, 42(2):215–20, 1998

[83] Feng, L., Li, S., Li, H., Zhai, J., Song, Y., Jiang, L., Angew Chem Int Ed, 41(7):1221–3, 2002

[84] Niu, Z., Bruckman, M., Kotakadi, V.S., He, J., Emrick, T., Russell, T.P., Yang, L., Wang, Q., Chem. Commun., 3019–3021, 2006

[85] Ellison, C.J., Phatak, A., Giles, D.W., Macosko, C.W., Bates, F.S., Polymer, 48, 3306-3316, 2007

[86] Formhals, A., Gastell, R. S., US Patent 1,975,504, 1934

[87] Deitzel, J. M., Kleinmeyer, J., Harris, D., Tan, N.C.B., Polymer, Vol. 42, 261 – 272, 2001

[88] Ko, F., "Nanofibre Technology: Bridging the Gap between Nano and Macro World." NATO ASI on Nanoengineeered Nanofibrous Materials, 2003

[89] Zhang, Y., Lim, C. T., Ramakrishna S., Huang, Z-M., Journal of Materials Science: Materials In Medicine, 16, 933– 946, 2005

90 Kim, C.-W., Frey, M. W., Marquez, Manuel, Yong, L. J., Journal of Polymer Science: Part B: Polymer Physics, Vol. 43, 1673–1683, 2005

91 Nevell, T. P., Zeronian, S. H., Cellulose Chmistry and Its Applications, 1985

92 Dawsey, T.R., McCormick, C.L., J. Macromol. Sci. – Rev. Macromol. Chem. Phys., C30: 405 -440, 1990

93 Fink, H.P., Weigel, P., Purz, H.J., Ganster, J., Progress in Polymer Science, 26, 1473-1524, 2001

94 Scheraga, H.A., J. Chem. Phys., 23, 1526-1531, 1955

95 Zhang, Y., Lim, C. T., Ramakrishna S., Huang, Z-M., Journal of Materials Science: Materials In Medicine, 16, 933– 946, 2005

96 Kulpinski, P., Journal of Applied Polymer Science, Vol. 98, 1855–1859, 2005

97 Viswanathan, G., Murugesan, S. Pushparaj, V., Nalamasu, O., Ajayan, P.M., Linhardt, R.J., Biomacromolecules, Vol. 7, No. 2, 2006

98 Kim, C.-W., Frey, M. W., Marquez, Manuel, Yong, L. J., Journal of Polymer Science: Part B: Polymer Physics, Vol. 43, 1673–1683, 2005

99 Carothers, W. H., Hill, J. W., Journal of American Chemical Society, 54, 1579-91 1932

100 Reneker, D. H., Chun, I., Nanotechnology, 7, 216, 1996.

101 Demir, M.M., Yilgor, I., Yilgor, E., Erman, B., Polymer, 43:3303–9, 2002

102 Fink, H.P., Weigel, P., Purz, H.J., Ganster, J., Progress in Polymer Science, 26, 1473-1524, 2001

103 Fink, H.P., Weigel, P., Purz, H.J., Ganster, J., Progress in Polymer Science, 26, 1473-1524, 2001

104 Fink, H.P., Weigel, P., Purz, H.J., Ganster, J., Progress in Polymer Science, 26, 1473-1524, 2001

105 Carrillo, F., Colom, X., Sunol, J.J., Saurina, J., European Polymer Journal 40 2229–2234, 2004

106 Nelson ML, O'Connor RT, J. Appl. Polym. Sci., 8:1311–24, 1964

107 Nelson ML, O'Connor RT., J. Appl. Polym. Sci., 8:1325–41, 1964

108 Marchessault, R.H., Liang, C.Y., J. Polym. Sci., 43:71–84, 1960

109 Klemm, D., Heublein, B., Fink, H.P., Bohn, A., Angewandte Chemie International Edition, 44, 3358 – 3393, 2005

[110] Bragg, W.L., Proceedings of the Cambridge Philosophical Society, 17, 43–57, 1913

[111] Lenz J, Shurz J, Wrentschur E., Acta Polym, 43:307–12, 1992

[112] Carrillo, F., Colom, X., Sunol, J.J., Saurina, J., European Polymer Journal 40 2229–2234, 2004

[113] Gennes, P.G.d., Reviews of Modern Physics, 57, 3 (part I), p.827-863, 1985

[114] Young, T., Phil. Trans. R. Soc. Lond. 95: 65–87, 1805

[115] Spelt, J.K., Neumann, A.W., Langmuir, 3 (4), pp 588–591, 1987

[116] Schurz, J., Acta Polym., 36, 80, 1985

[117] Hamad, W.Y., Journal of Materials Science Letters, 17, 433-436, 1998